

博士論文

Ph.D. Thesis

EOG 計測を用いたロボット操作法の開発

Development of Robot Operation Method
using Electrooculography(EOG) Measurement

Year 2020 (2020 年)

MUHAMMAD SYAIFUL AMRI BIN
SUHAIMI

Acknowledgment

Many experiences and knowledge that I have learned during the 6 years of studies in Sasaki and Matsushita laboratory. I have been accepted as a laboratory member since I am an undergraduate student in 2014 and finally given opportunities to finish my studies as a Ph.D. student in 2020.

For that, I would like to express my highest gratitude toward my main supervisor, Professor Minoru Sasaki, and co-supervisor, Professor Kojiro Matsushita for their kind support and guidance. I also would like to extend my gratitude toward Professor Satoshi Ito and Professor Tetsuya Mouri for greatly assisted in the research. Without their humble support, I would not be able to achieve a step in my future life dream which is to be a university professor.

Then, I would like to express my gratitude to all my laboratory colleagues. Notably, the Ph.D. students that have graduated from the laboratory and those currently still studying hard in Ph.D. studies. Those mentioned include; Muhammad Ilhamdi Rusydi(2014), Harrison Ngetta(2014), Meisam Taheri(2017), Waweru Nyeri(2019), Titus Murwa(2019), Pringgo Widyo Laksono, and Muguro Joseph.

I also want to include my gratitude to the organizations that I received sponsorship during my studies at Gifu University. Jabatan Perkhidmatan Awam(JPA) from Malaysia has supported me during my undergraduate studies(the Year 2010 – 2015). Gifu University has supported me with tuition waivers during my master studies(the Year 2015-2017). Finally, Yayasan Pelajaran Mara(YPM) under the Malaysia Japan High Education Program(MJHEP) from Malaysia for supporting my Ph.D. studies(the Year 2017 - 2020).

Abstract

Non-physical interaction has been an interest in the control method in recent years. The conventional control methods that rely on hand and leg manipulation are incapable to be used for those who are physically disabled. Physically disabled people such as Amyotrophic lateral sclerosis(ALS) patients are paralyzed from neck to toe. They are constrained to do interaction by using their eye, mouth or head movement. Thus, we proposed using the bio-signals interaction method and we focus on the Electrooculography (EOG).

The research goal of this paper is to develop an EOG control method for robot operation. We have successfully enhanced the EOG measurement by increasing the signal measurement stability for the EOG gaze direction and improved EOG gaze estimation accuracy by proposing a calibration method. Other than that, we also able to determine which eye gaze methods; gaze direction or gaze estimation is the best for robot control operation.

In this research, the EOG eye gaze is discriminated into 3 types; gaze direction and gaze estimation, and eye blink. The gaze direction is successfully discriminated against to 8-directions by using maximum and minimum signal amplitude polarity. The gaze estimation is discriminated against by the computation of the signal integral. Inside the eye blink discrimination, there are two types of eye blink; voluntary and involuntary blink. The voluntary eye blinks can be discriminated by the value of the maximum and minimum amplitude value of the Ch2 signal. The amplitude has a higher value compared to other eye gazes. On the other hand, the involuntary blink is discriminated against by the Ch2 signal maximum and minimum amplitude time width. The involuntary blink is

an instantaneous eye motion in nature, so the time width is significantly shorter compared to other eye gazes.

There are other methods implemented to support eye gaze EOG control. EMG bite is used to increase the eye gaze control inputs. The EMG bite is successfully discriminated by using the signal differential computation. The EMG produced a differential value higher than other eye gazes. Then, color-based image processing is used to assist the gaze estimation measurement. By computing a target object center point and compared with the gaze estimation, the object selection accuracy is improved.

There are three objectives of this research. The first objective is to enhance the EOG measurement stability for eye gaze. A custom-made EOG mask is proposed. An investigation on EOG signal stability is conducted to compare the conventional manual hand electrode placement and the proposed method. Three times eye gaze directions(up, down, right, and left) are measured. The signal pattern, maximum amplitude consistency, and signal standard deviation are investigated. From the experiment, the proposed method has the best results. Thus, we understood that the signal for the EOG mask is more stable.

The second objective is to enhance the accuracy of the EOG gaze estimation method using the calibration method. We proposed the conversion method for 24-point gazing data simultaneously and assumed a virtual origin (i.e., 25th point) on gaze coordinates with 24-point gazing data and applied an affine transformation to 24-point gazing data. Two sub experiments were conducted as a comparative investigation for the conventional and proposed methods. The first sub experiment was an accuracy investigation between the proposed method and conventional computation. The second sub experiment was to determine the accuracy of the proposed method using EOG gazing data. Both experiment results show that the proposed method has the best result. Thus, EOG gaze estimation

accuracy is enhanced by the proposed method.

The final objective is to compare which EOG gaze method; EOG gaze direction or gaze estimation performs better for robot control. There are four sub experiments have been conducted. The first sub experiment is to investigate the accuracy of gaze estimation with the support of image processing. The image processing is used to determine an object center point and the accuracy is determined with the distance(error distance) between the gaze estimation and the object center point. The result shows that the error distances are in the range of 1.5 to 3.0 [cm]. The distance then is used to create a circular area from the object center point. If the gaze estimation is in the area, the object is assume selected and the robot arm moved to the object center point position. The second sub experiment is to investigate the gaze estimation method for object displacement task. Two error distances from the previous result are used; 2 and 3[cm]. The two distances are investigated to determine if the control performance improved when the distance parameter changed. From the result, the 3[cm] error distances show the best time for the object displacement task. The third sub experiment is to investigate the gaze direction method for object displacement task. Each eye gaze direction manipulates the direction of the robot arm movement. There are two distances for the robot arm movement; 2 and 3 [cm] proposed. Similar to the gaze estimation method, the two distances are investigated to determine the control performance improved if the distance parameter changed. From the result, the 3[cm] robot movement shows the fastest time. The fourth sub experiment is to compare the two gaze methods to determine which gaze method is the best for robot control. Using second and third sub experiment results, the gaze estimation shows the best result. Thus, the robot control for EOG is the best by using gaze estimation.

Table of Contents

Acknowledgment	1
Abstract	2
Chapter 1	Introduction	7
Chapter 2	Methodology	
2.1	Hardware and Software	
2.1.1	EOG and EMG measurement device	10
2.1.2	Microsoft Visual Studio C/C++	13
2.1.3	MATLAB	14
2.2	Electrode Attachment Method	15
2.3	Electrode Attachment Mask (EOG Mask)	16
2.4	EOG and EMG Discrimination	
2.4.1	Gaze Direction	20
2.4.2	Gaze Estimation	22
2.4.3	Eye Blink	24
2.4.4	EMG Bite	28
2.5	Coordinate Transformation Method	30
2.6	Color-based Image Processing	34
Chapter 3	EOG measurement stability (EOG mask)	
3.1	Background	36
3.2	Experiment:	37
3.2.1	Investigation on EOG signal stability for conventional electrode attachment and EOG mask	39
3.3	Discussion	42

Chapter 4	Calibration method for AC-EOG Gaze Estimation	
4.1	Background	43
4.2	Experiment	46
4.2.1	Investigation on Coordinate Transformation for Cross-shaped electrode attachment method	47
4.2.2	Investigation on Cross-shaped electrode attachment and Plus-shaped electrode attachment to the AC-EOG Accuracy	50
4.3	Discussion	59
Chapter 5	Robot Control based on EOG Gaze Direction and Gaze Estimation	
5.1	Background	61
5.2	The proposed robot control system	
5.2.1	Experiment setup	63
5.2.2	Proposed EOG and EMG control method	66
5.2.3	Robot control process	69
5.3	Experiment	
5.3.1	Investigation on Gaze Estimation Accuracy using Color-based Image processing	71
5.3.2	Performance Investigation on Gaze Estimation to the Object Displacement Task.....	73
5.3.3	Performance Investigation on Gaze Direction for the Object Displacement Task.....	79
5.3.4	Performance comparison between EOG gaze direction and gaze estimation methods	85
5.4	Discussion	88
Chapter 6	Conclusion	91
Reference	95
List of Publications	100

Chapter 1

Introduction

Non-physical interaction has been an interest in the control method in recent years. The conventional control methods commonly use hand or leg manipulation. Taking the computer control as an example, the user needs to use hand to move the mouse and keyboard typing. While these methods are accessible for most people, those who are physically disabled will face difficulties.

Physically disabled people such as Amyotrophic lateral sclerosis(ALS) patients are paralyzed from neck to toe. They are constrained to do interaction by using their eye, mouth or head movement. With the limited interaction methods, we believe the eye is of the best choice to be used for non-physical control. The high degree of freedom of the eye movement could offer more control capability compared to others.

One of the methods to detect eye movement is by using bio-signal analysis and Electrooculography(EOG) is the method[1]. The EOG signals are electrical potentials produced when the eyeball moves. Imagine the eyeball as similar to a battery, where the eye cornea provides the positive potential and the eye retina provides the negative potential [2]. For that reason, it is possible to estimate eye movements by analyzing the resulting EOG signals.

Then, there are two types of EOG analysis methods: Direct-current-EOG (DC-EOG) and alternating-current-EOG (AC-EOG). DC-EOG signals are the basis for the EOG signal which is an almost raw signal with the amplitudes that are directly related to the

eye movement [3]. DC-EOG has a disadvantage in that the resulting signals are easily influenced by human movement. A motion restriction is required to ensure precise measurement [4-5]. On the other hand, AC-EOG is a DC-EOG which has been augmented with a band-pass filtered DC-EOG and is strongly against human movements.

In the conventional EOG electrode attachment method, the electrodes are attached for specific locations around the eye by hands. However, there are correlations that the EOG signal is affected by the electrode attachment method. M. Yan et al. [6] and Aungsakun et al.[7] shows that different position gives different signal characteristics. Thus, electrode attachment is one of the major considerations for signal measurement. Even though the same locations are used, precision and consistency in electrode placement are the requirements to have measurement stability.

As for EOG for control, the discrimination is based on two methods; gaze estimation and gaze direction. Gaze estimation is a method to determine the eye gazing position. Ilhamdi et al. [8-10] studied the application of EOG gaze estimation for robot control. Four electrodes were attached around the user's eyes in the cross-shaped arrangement. However, gaze estimation discrimination requires a calibration method to the signal. The user is required to gaze at several target points, and each signal is used for determining the conversion parameters from eye moment and gaze estimation at the calibration phase. The calibration is the most important factor since it adjusts individual differences or the electrode attachment method.

On the other hand, the gaze direction is a method to determine the direction of the eyeball movement. Compared with the gaze estimation, this method is more common to be used for control. The reason that is the gaze direction could offer a simpler signal discrimination method, i.e. signal amplitude polarity with higher accuracy[11-12].

Therefore, most of the EOG based application from this method. There are PC interface operation [13-19], robot arm operation [20-23], and electrical wheelchair operation [24-25]. Although, a thorough comparison between gaze direction and gaze estimation for robot control to do the same task is an interesting topic to be explored.

The research goal of this research is to develop a robot operation method using Electrooculography(EOG). There are three objectives; (1) to increase the EOG measurement stability, (2) to improve the accuracy of gaze estimation by calibration method, and (3) to determine which eye gaze methods; gaze direction or gaze estimation methods are the best for robot control. From the objectives, we are expecting the EOG for robot control is stable and accurate. Then, we also expect to search for the best eye gaze methods for robot control.

The chapter writing structure in this thesis based on the research objectives and its related information. There are seven chapters in this thesis. In chapter 1, we will explain the problem statement and the objectives of the research. In chapter 2, we will explain the research methodology. Every information on research equipment, software, discrimination method, and other methodologies are discussed in detail. Chapter 3 is the first experiment in which we proposed an EOG mask as an electrode placement improvement method. An investigation on EOG signal stability is conducted. Chapter 4 is the second experiment where we proposed a coordinates transformation calibration to improve gaze estimation precision. Chapter 5 is the third experiment where a comparison between gaze direction and gaze estimation for robot control is conducted. An object displacement task using a 3D robot arm is proposed, the time of task completion is used as the basis of the investigation.

Chapter 2

Methodology

2.1. Hardware and Software

2.1.1. EOG and EMG Measurement device

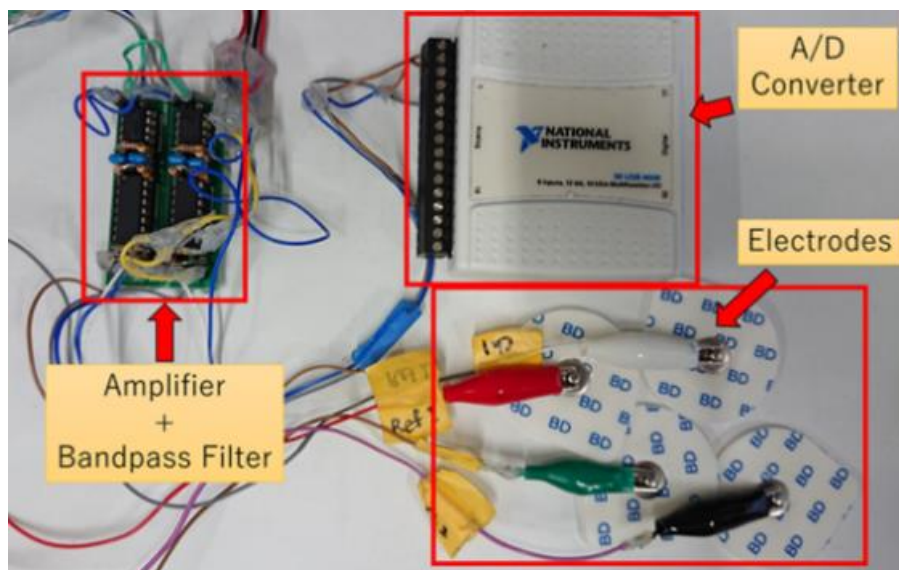


Figure 1. EOG and EMG measurement device.

A low-cost EOG and EMG measurement system are developed for the research. The photo of the system shown in Figure 1. In this system, four main components are set-up: Disposable electrodes, an EOG and EMG measurement circuit (comprising of a differential amplifier, bandpass filter, and an inverting amplifier, all connected in cascade), a data acquisition device (National Instruments (NI) Corporation USB-6008), and a PC running Windows 10. Figure 2 shows the system process and the measurement circuit

schematic. The function of each component is as such;

1. **Disposable electrodes:** Measuring Direct-Current-EOG(DC-EOG) from the eyeball movement as the input signal. The input DC-EOG from the eye is relatively small.
2. **EOG measurement circuit:** Amplifying the input signal to the designated range. A bandpass signal filtering method is also applied to convert the input DC-EOG signal into Alternate-Current-EOG(AC-EOG) signal. In the research, we are utilizing the AC-EOG form of signal for EOG discrimination.
3. **A/D converter:** Convert the amplified AC-EOG signal from the circuit into binary data. The binary conversion is to enable us to analyze the signal on a computer.
4. **Computer:** Analyze the EOG and EMG signal for discrimination and data saving.

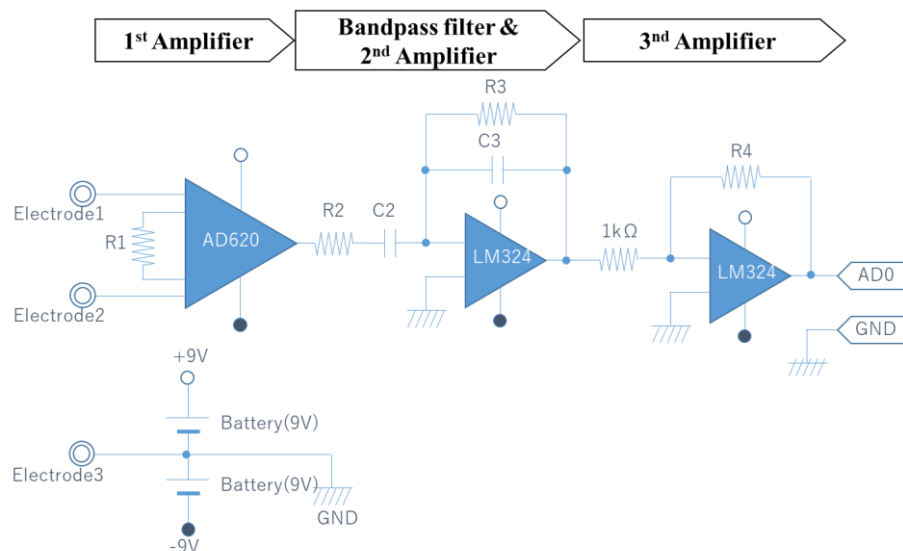
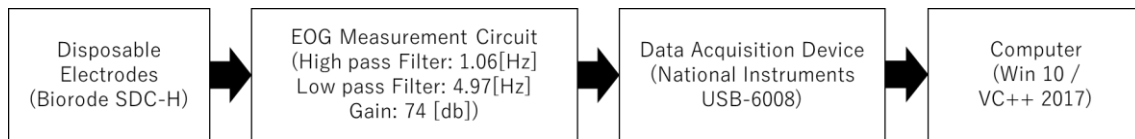


Figure 2. EOG and EMG measurement processes and circuit schematic

Table 1: The amplification value and the gain for EOG and EMG measurement.

Content	1 st amplifier	Bandpass 2 nd Amplifier					3 rd amplifier	Final Output	
	Capacitor Value R1[Ω]	Filter type	Cut-off Frequency [Hz]	Resistor Value (R2/ R3) [Ω]	Capacitor Value [F]	[uF]	Resistor Value (R5/R4) [Ω]	Amplification factor	Gain [db]
Value	1000	High-pass	1.06	15000	0.00001	10	750000	7912	78
		Low-pass	4.97	3200	0.00001	10	1000		
Amplification factor	49.4	0.21			750.0				

The EOG system is configured as two channels (Ch1 and Ch2). Based on table 3, the system has a bandpass filter which a lower cut-off frequency of 1.06 Hz and an upper cut-off frequency of 4.97 Hz is set. This filter is used to convert the DC-EOG to AC-EOG. The gain for the system is 78[db] with sampling frequency in the data acquisition device is 1 kHz.

2.1.2. Microsoft Visual Studio C/C++

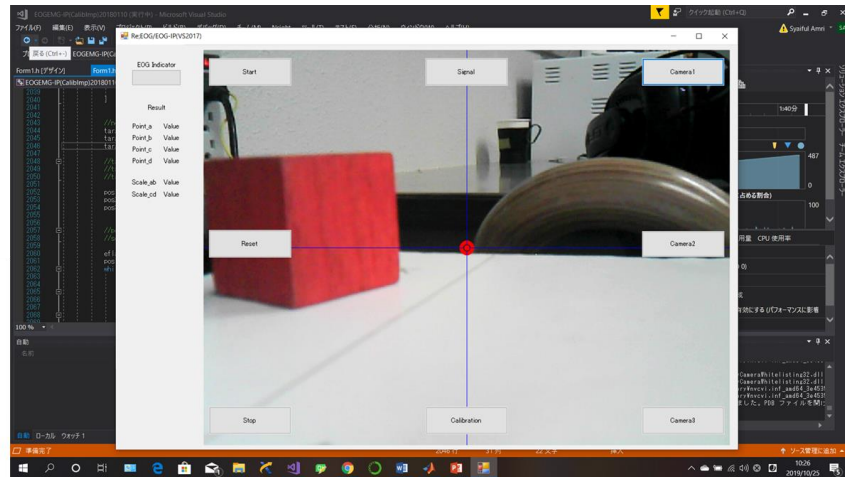


Figure 4. Development of Camera Interface using Microsoft Studio C++ 2017

The robot operation based on EOG has been developed using Visual Studio software from Microsoft. We have chosen the visual studio C/C++ 2017 version as the programming platform. The C/C++ based programming is an optimal choice in reading the EOG and EMG signal data from the National Instrument(NI) data acquisition Device. Besides, the software is supported to capture camera image and image processing by including OpenCV libraries. Figure 4 shows the image of a running camera interface using visual studio C/C++ 2017.

2.1.3. MATLAB

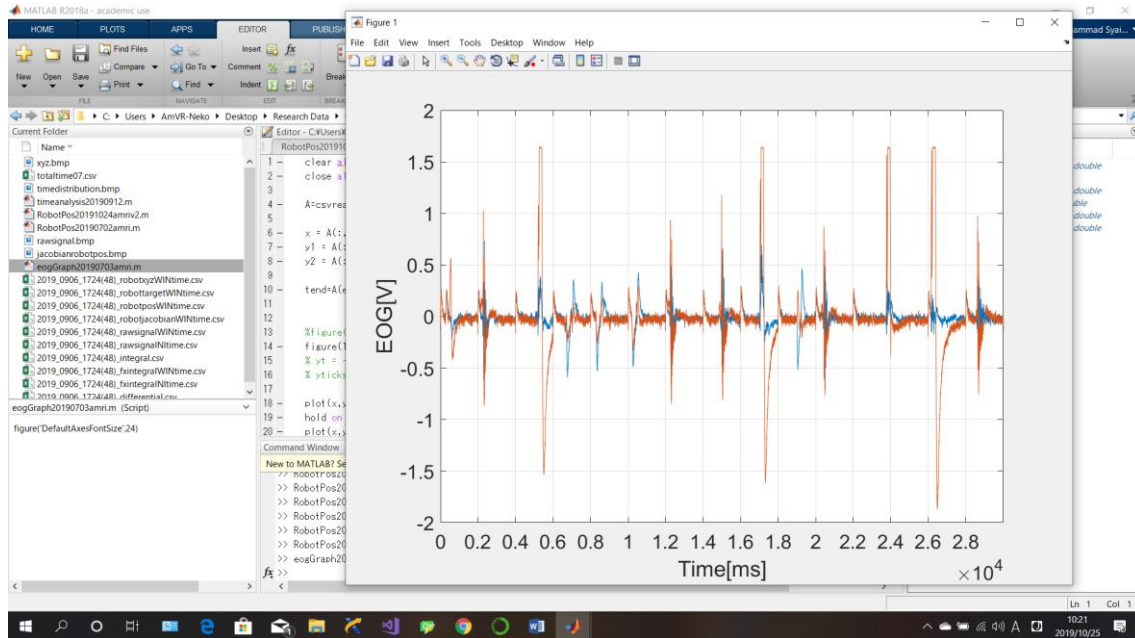


Figure 5. Graph Plotting using Matlab 2017b

Matlab has been used primarily to analyze the EOG and EMG data. The abundance in mathematical functions in Matlab made the data analysis became simple and easy. Moreover, Matlab offers an interactive graph plotting. All experimental graph shown throughout the paper is based on Matlab graph plot. Figure 5 shows the image of the graph plotting on the Matlab.

2.2. Electrode Attachment Method

There are two major electrode attachment shapes implemented for the experiment. The arrangement is as shown in Figure 6: One is the plus-shaped five-electrode arrangement, and the other is the cross-shaped four-electrode arrangement. The plus-shaped type is suitable for recording EOG signals generated by vertical eye movements and horizontal eye movements since the electrodes are attached in the same direction. Meanwhile, the cross-shaped type has the advantage of a smaller number of electrodes. However, the technique requires appropriate post-processing conversion of EOG signals to gaze position.

There is a notable point need to be considered during placing each electrode around the eye. The electrode needs to be carefully placed as to parallel to the eye center. By carefully attach the electrode, we could standardize the electrode placement for the test subject in experiments and reduce the inconsistency of the signal to be analyzed.

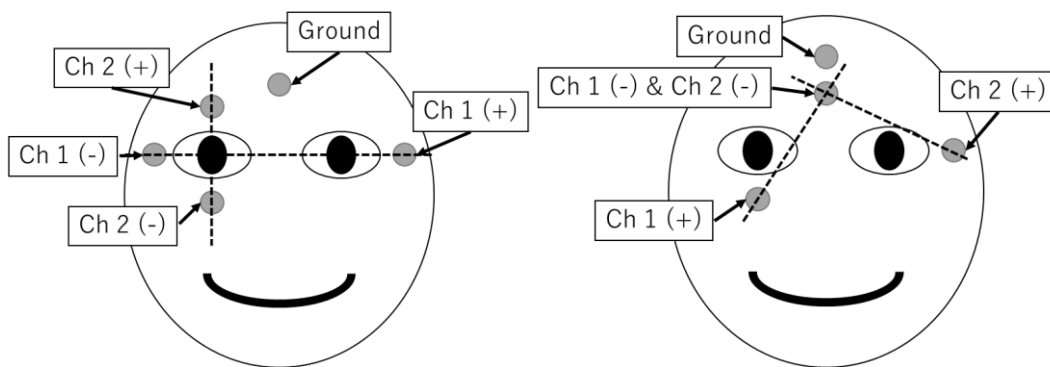


Figure 6. (a) Plus-shaped electrode attachment and (b) cross-shaped electrode attachment.

2.3. Electrode Attachment Mask (EOG Mask)

The conventional EOG attachment method is time-consuming and requires precision to attach the electrode parallel to the eye center. To simplify the electrode attachment, we develop a new method in which we manufacture an EOG face mask with precise electrode placement designed.

To make the mask, we are using 3 types of equipment; 3D scanner from Creaform Co., Ltd. Go! Scan 3D, 3D model editing software from Materialise Co., Ltd 3-Matic and 3D printer. Several processes are necessary for manufacturing the EOG mask, the processes are;

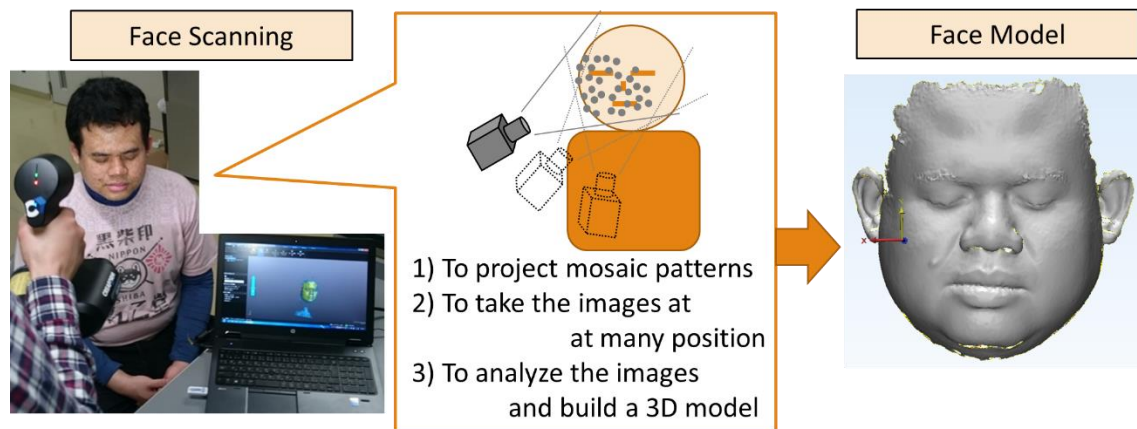


Figure 7: Face scanning process

- (1) Figure 7 shows the first process. The face-scanning process required two-person. Using the 3D scanner, the test subject face is scanned several times at different angles to obtain the detailed information of the face. The information then converted into a face model.

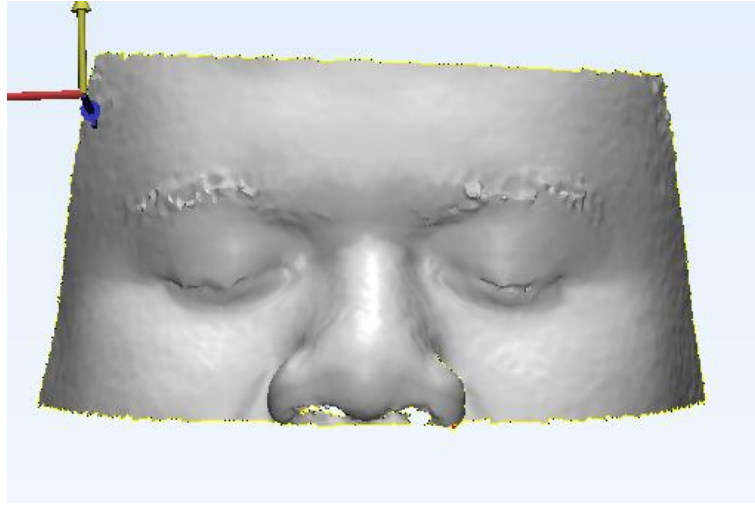


Figure 8. Face model extraction process

- (2) The second process is the face model extraction process. The region of interest for the proposed mask is the region surrounding the eye. As such, mouth and some parts of the forehead region are removed from the face model. Figure 8 shows the region of the interest extraction process.

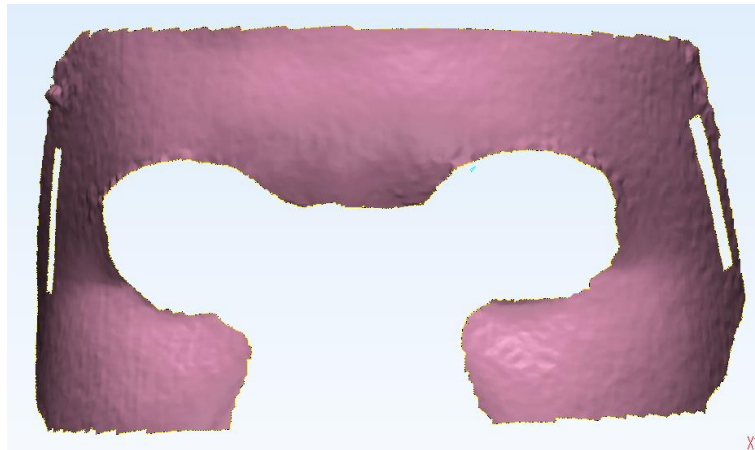


Figure 9. Face model cutting process

- (3) The thirds process is to remove the eye and the nose area. Considering the mask to be mount on the face for the research, the eye and nose will be an obstruction. The eye and nose removal process is as shown in Figure 9.

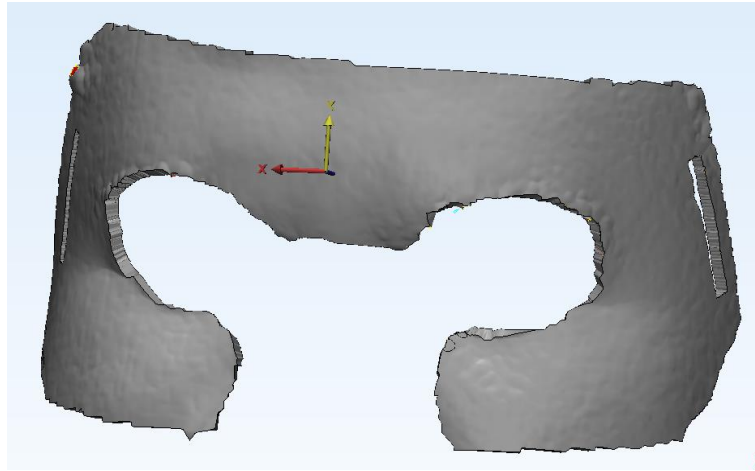


Figure 10. Face model Thickening process

- (4) To manufacture the EOG mask using the 3D printer, a thickening process for the face model is required. Forth process is the thickening process. Figure 10 shows the process.

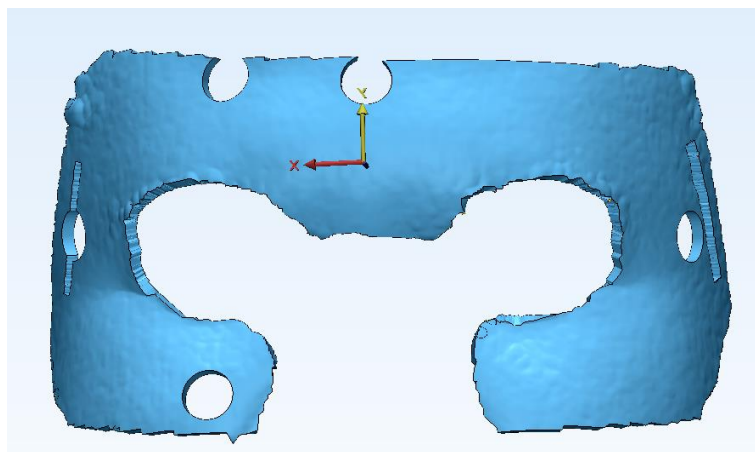


Figure 11. Electrode positioning on mask process

- (5) The fifth process is to modify the mask for the electrode attachment position. 5 designated hole positions are removed from the face mask as shown in figure 11.

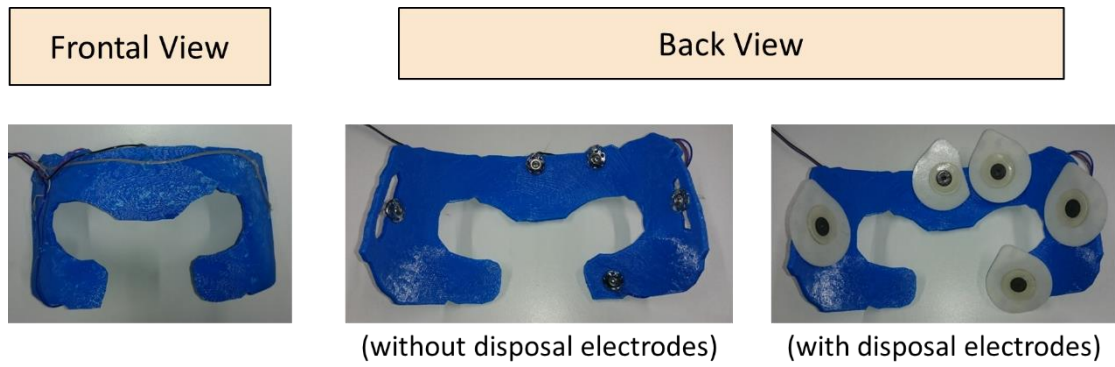


Figure 12. Face mask manufacture process

- (6) The last process is to manufacture the face mask. A 3D printer is used to manufacture the mask based on the edited face model from previous processes. The manufactured EOG mask is as shown in figure 12.

2.4. EOG and EMG Discrimination

2.4.1. Gaze Direction

For the EOG gaze direction, we are proposing discrimination for 8-directions(Up, Down, Right, Left, Up-right, Up-left, Down-right, and Down-left) from the eye movement. Two EOG channel (Ch1 and Ch2) signals are discriminated against to determine the gaze direction. From the signals, we proposed an amplitude polarity technique to analyze the EOG signal.

In determining the polarity, we included two signals analysis method. First, The polarity is determined by the signal amplitude that exceeds the threshold value. The positive polarity is determined if the amplitude above the positive threshold and the negative polarity is determined if the signal amplitude below a negative threshold. The threshold is implemented to remove residue noises from the discrimination. Noises in signal disrupt the accuracy of gaze direction discrimination.

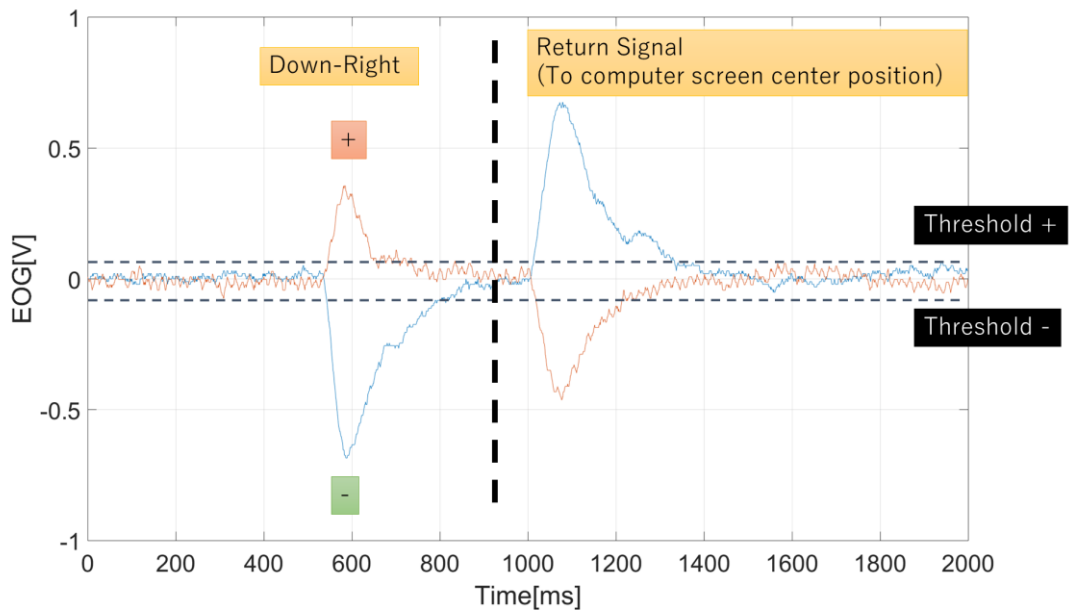


Figure 13. Ch1 and Ch2 discrimination method for gaze direction.

Second, we considered the EOG gaze direction from one direction signal and return signal. In the experiment, the test subjects start the gaze direction from the center of the monitor screen. After the desired gaze direction achieved, the test subject needs to return the gaze to the monitor center position. However, for polarity discrimination, we only discriminate the first half of the signal. This technique is implemented to discriminate gaze direction with voluntary eye blink that we will discuss in-depth later in methodology. Figure 13 shows examples of gaze direction discrimination.

Figure 14 shows the signal patterns for the whole 8-directions. Based on the figure, we observed that each direction has its distinctive pattern. With the first half signal amplitude discrimination method, we compute the 8-direction amplitude polarity in table 2.

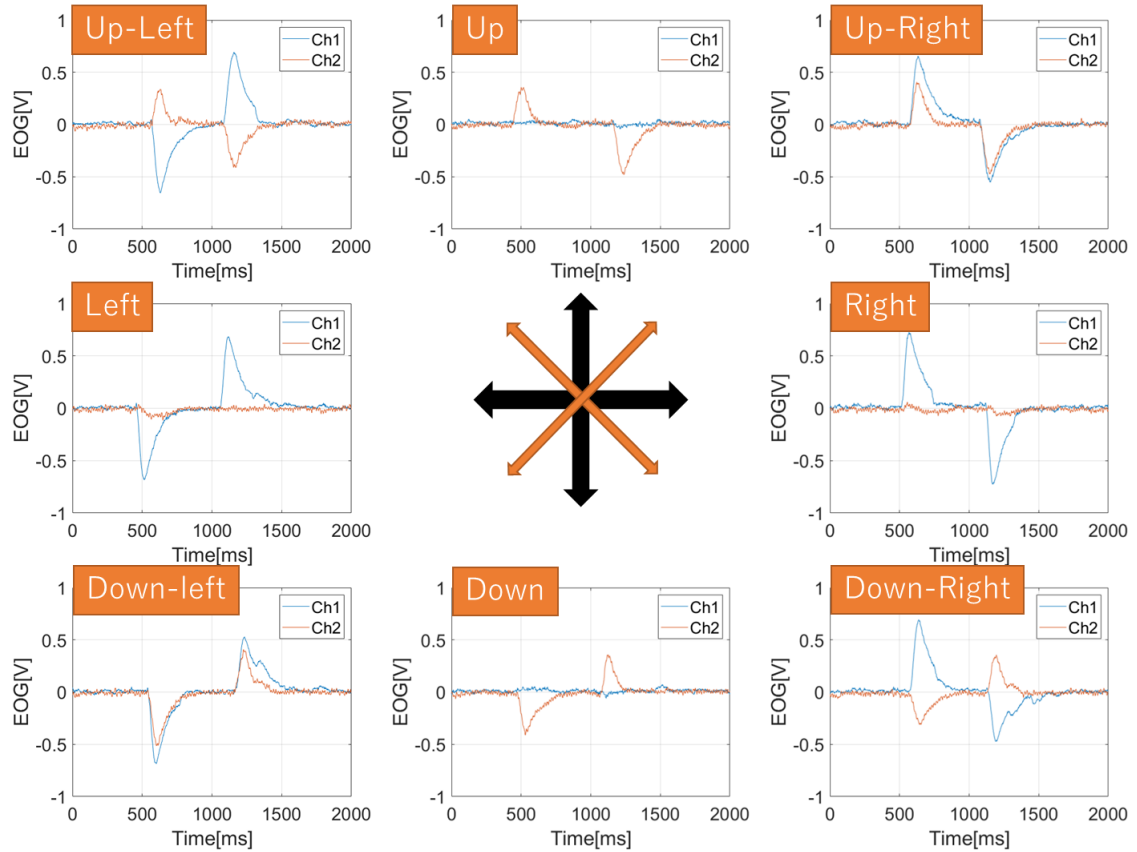


Figure 14. Gaze direction signal pattern and first half amplitude polarity.

Table 2. 8-Directions first half signal amplitude polarity

	Up	Down	Right	Left	Up - Right	Up - Left	Down - Right	Down - Left
Ch1	0	0	+	-	+	-	+	-
Ch2	+	-	0	0	+	+	-	-

2.4.2. Gaze Estimation

For the research, we determined the gaze estimation by analyzing the two EOG channel (Ch1 and Ch2) signals. The gaze estimation refers to the estimation of the points in space where the eyes of the subject are focused. In other words, it is the determination of the x and y coordinates on a two-dimensional plane.

From the signals, we proposed an integral method to analyze the EOG signal. In the integral computation, we included the signal thresholds method for Ch1 and Ch2 signals. The signal threshold served two purposes. The first purpose was to determine the polarity of the integral value. Positive integral was determined if the signal was above the positive threshold (th+) and negative integral was determined if the signal was below the negative threshold (th-). Second, the thresholds were introduced to remove any unwanted residual noises from the integral value, as noises could affect the accuracy of gaze estimation. The equation to obtain the signal integral is derived as equation (1)-(4).

$$EOG_{\text{integral}_{ch_i}} = \left| \int_{th_p} EOG_{ch_i}(t) dt \right| + \left| \int_{th_n} EOG_{ch_i}(t) dt \right| \quad (1)$$

$$th_p = \{t: EOG_{ch_i}(t) > th +\} \quad (2)$$

$$th_n = \{t: EOG_{ch_i}(t) > th -\} \quad (3)$$

$$i = 1,2 \quad (4)$$

Figure 15 shows an example of EOG analysis for integral value. Then, to determine the gaze estimation for x and y coordinates, the x value is represented by the channel Ch1 integral value and y value from channel Ch2 integral value.

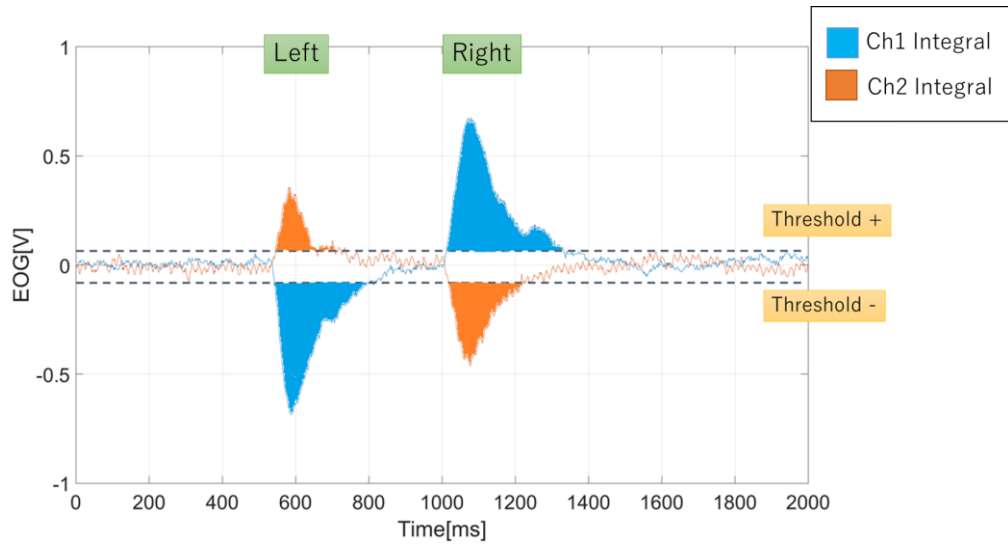


Figure 15. Signal integral method for left and right eye movement.

2.4.3. Eye Blink

Eye blinking shared a signal similarity with up eye gaze. During eye blinking, the eyeball saccade toward upward and return to the original eye position before blinking. Moreover, there are two different types of eye blink; voluntary blink and involuntary blink. Involuntary blink is defined by unconscious blinking that human does to retain humidity in the eyeball. Meanwhile, voluntary blink is a motion that we purposely blinking our eyes.

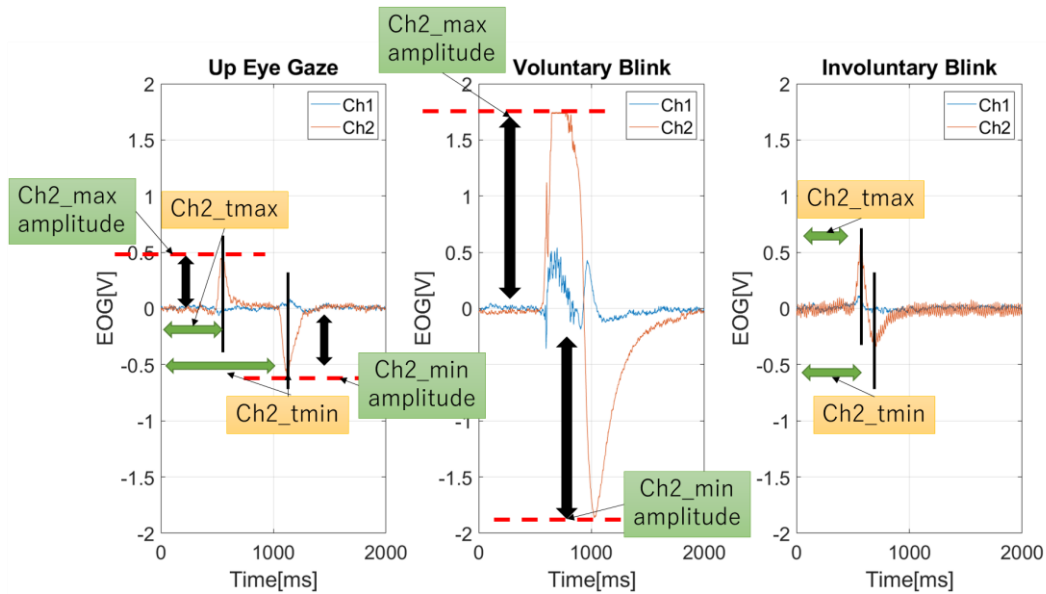


Figure 16. Up eye gaze, voluntary blink, and involuntary blink signals

Figure 16 shows the difference in EOG for up eye gaze, involuntary blink, and voluntary blink. We observed that voluntary and involuntary eye blinks are discriminated with the amplitude value and time widths. Ten samples were obtained for the voluntary blink and voluntary blink discrimination. Table 3 shows the signal amplitude for each up

eye gaze, voluntary blink and, involuntary blink. From the table, involuntary blink produced a higher signal amplitude in comparison with the others. Thus, as involuntary discrimination, we discriminate the signal maximum amplitude to exceed 1.5[v] and -1.5[v].

Table 3. Average signal amplitude computation for up eye gaze, involuntary blink, and involuntary blink

No.	Up Eye Gaze		Voluntary Blink		Involuntary Blink	
	Ch2 max[v]	Ch2 min[v]	Ch2 max[v]	Ch2 min[v]	Ch2 max[v]	Ch2 min[v]
1	0.1818	-0.135	1.7451	-1.7801	1.1525	-0.5846
2	0.2942	-0.4313	1.7451	-1.7903	0.6620	-0.3904
3	0.4679	-0.5948	1.7451	-1.8618	0.5700	-0.3394
4	0.1511	-0.2576	1.7451	-1.8925	0.6211	-0.2883
5	0.3350	-0.3598	1.7451	-1.8414	0.6109	-0.2985
6	0.4883	-0.4722	1.7451	-1.8823	0.3657	-0.1657
7	0.0387	-0.0839	1.7451	-1.9538	0.3861	-0.4109
8	0.0694	-0.0941	1.7451	-1.9129	0.4883	-0.2372
9	0.0694	-0.0941	1.7451	-1.9027	0.7642	-0.3291
10	0.0591	-0.0635	1.7451	-1.9947	0.4066	-0.2065
Ave.	0.21549	-0.25863	1.7451	-1.8813	0.60274	-0.32506

As for voluntary blink, we are determining the discrimination method from signal amplitude time width. Involuntary eye blink naturally produced maximum and minimum signal amplitude similar to up eye gaze and return signal. The time width calculated from the time difference between the maximum amplitude and minimum amplitude. Tables 4 shows the difference between the signal amplitude time position. Then, using equation(5), we compute the time-width between the maximum and minimum signal amplitude.

$$\text{timewidth} = \text{Ch2min}_{\text{time}} - \text{Ch2max}_{\text{time}} \quad (5)$$

Ch2min_time = Ch2 signal minimum amplitude time

Ch2max_time = Ch2 signal maximum amplitude time

Table 5 shows the result of the time-width computation. From the computation, the voluntary eye blink produced minimal time-width in comparison to up eye gaze and involuntary blink. Voluntary blink is an instantaneous motion, it took less than 200[ms].

Table 4. Ten samples of signal maximum and minimum amplitude time position for up eye gaze, involuntary blink, and involuntary blink

No.	Up Eye Gaze		Voluntary Blink		Involuntary Blink	
	Ch2max_ Time[ms]	Ch2min_ Time[ms]	Ch2max_ Time[ms]	Ch2min_ Time[ms]	Ch2max_ Time[ms]	Ch2min_ Time[ms]
1	577	1134	478	870	373	515
2	567	1060	600	1023	512	637
3	545	1050	649	1025	565	707
4	530	1090	598	993	401	509
5	559	1066	602	997	569	694
6	582	1006	572	942	586	678
7	646	1189	849	1248	453	678
8	637	1162	576	960	369	477
9	686	1211	783	1143	301	426
10	460	1117	727	1127	452	594

Table 5. Average of ten samples of time-width computation for up eye gaze, involuntary blink, and involuntary blink

No	Up Eye Gaze	Voluntary Blink	Involuntary Blink
	Time Width[ms]	Time Width[ms]	Time Width[ms]
1	557	392	142
2	493	423	125
3	505	376	142
4	560	395	108
5	507	395	125
6	424	370	92
7	543	399	225
8	525	384	108
9	525	360	125
10	657	400	142
Ave.	529.6	389.4	133.4

2.4.4. EMG Bite

The EMG in this research is additional support for EOG based control. We obtained the EOG from mouth biting motion which measured with the same measurement system for the EOG. Figure 17 shows the signal pattern for EMG bite in comparison with the EOG signal from eye gaze and blinking. The EMG signal pattern has a distinctive pattern.

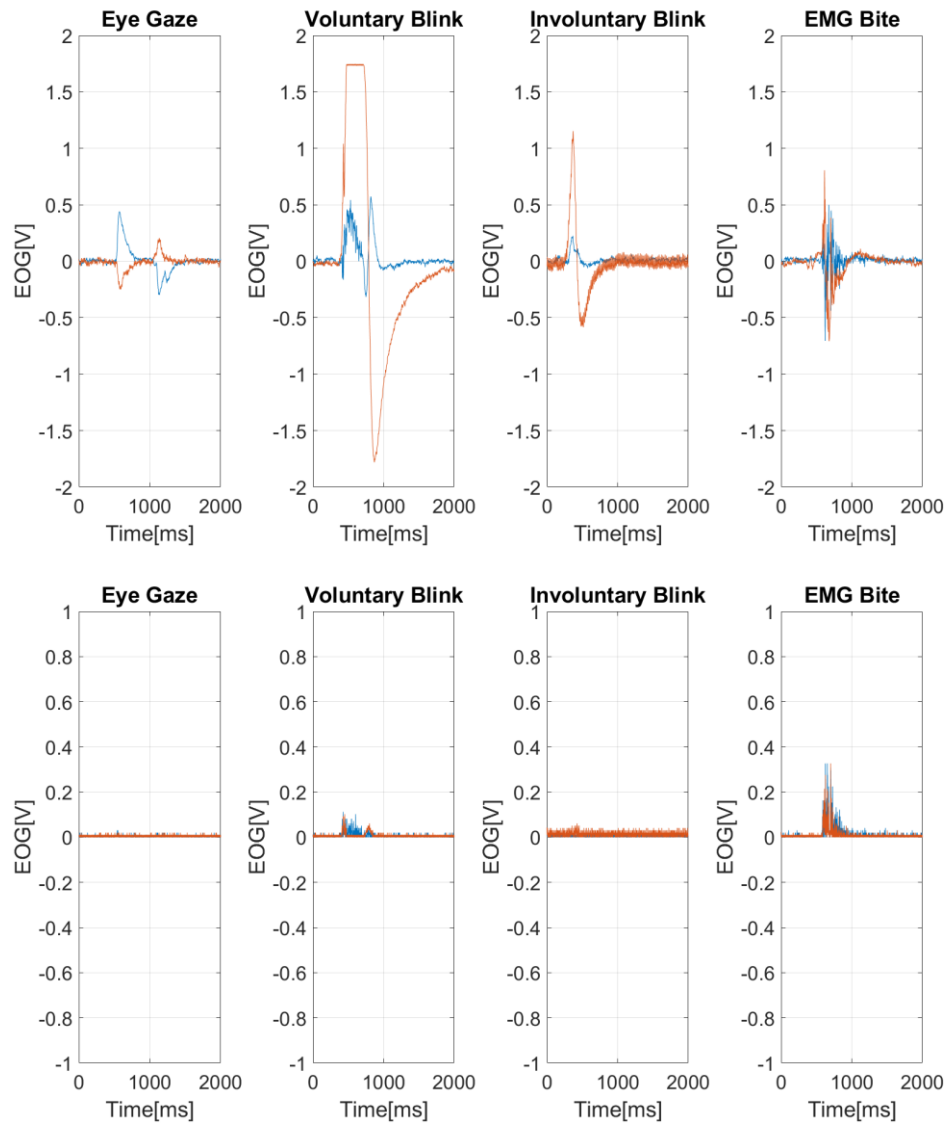


Figure 17. Up eye gaze, Involuntary blink, and voluntary blink and EMG bite signals(up) and absolute differential signals(down)

For EMG discrimination, a signal differential method is proposed. There are two processes in the signal differential method. The first process is to convert the signal using differential computation. Then, the differential conversion results are computed to have the absolute value. The EMG discrimination is based on the absolute maximum amplitude of the differential signal. Ten samples of random eye gaze, voluntary blink, involuntary blink, and EMG bite are taken to investigate the discrimination. Table 6 shows the results. Based on the table, the EMG bite produced a higher amplitude. The EOG has less amplitude value of 0.1[v] whereas EMG bite has amplitude more than 0.2[v].

Table 6. Ten samples of maximum differential value for eye gaze, involuntary blink, voluntary blink, and EMG bite.

No.	Eye Gaze		Voluntary Blink		Involuntary Blink		EMG Bite	
	Ch1	Ch2	Ch1	Ch2	Ch1	Ch2	Ch1	Ch2
1	0.0307	0.0204	0.1124	0.1022	0.1124	0.1022	0.3270	0.3270
2	0.0307	0.0307	0.1226	0.1124	0.1226	0.1124	0.2963	0.2963
3	0.0409	0.0204	0.1226	0.1431	0.1226	0.1431	0.3576	0.2452
4	0.0307	0.0328	0.1022	0.1124	0.1022	0.1124	0.2554	0.2657
5	0.0307	0.0307	0.1124	0.1124	0.1124	0.1124	0.5211	0.2759
6	0.0409	0.0328	0.1226	0.0817	0.1226	0.0817	0.5415	0.2350
7	0.0204	0.0307	0.1226	0.1124	0.1226	0.1124	0.2759	0.2146
8	0.0307	0.0204	0.0920	0.1022	0.0920	0.1022	0.3678	0.1941
9	0.0307	0.0226	0.1022	0.092	0.1022	0.0920	0.2657	0.2248
10	0.0307	0.0226	0.1124	0.1124	0.1124	0.1124	0.2248	0.2861
Ave	0.0310	0.0260	0.1100	0.1000	0.1100	0.1000	0.3400	0.2600

2.5. Coordinate Transformation Method

An interface for eye gazing target is used to investigate the gaze estimation. Using the EOG signal integral computation, an ideal gaze estimation result is that the gaze estimation has similar coordinates value as gaze target, as shown in Figure 18. To clarify the coordinate's position, we divided the coordinates into 4 sectors with different colors. In the previous studies using the cross-shaped electrode attachment, there is a significant problem with the accuracy between gazing data and targets [21]. Figure 19 shows the estimated gazing data obtained using the cross-shaped electrode arrangement. It can be observed that the estimated coordinates are rotated relative to the axes. We hypothesis that the rotation is caused by the shape of electrode attachment; cross-shaped. If the electrode attachment shape is transformed into plus-shaped, we expect there are no significant coordinate's rotation.

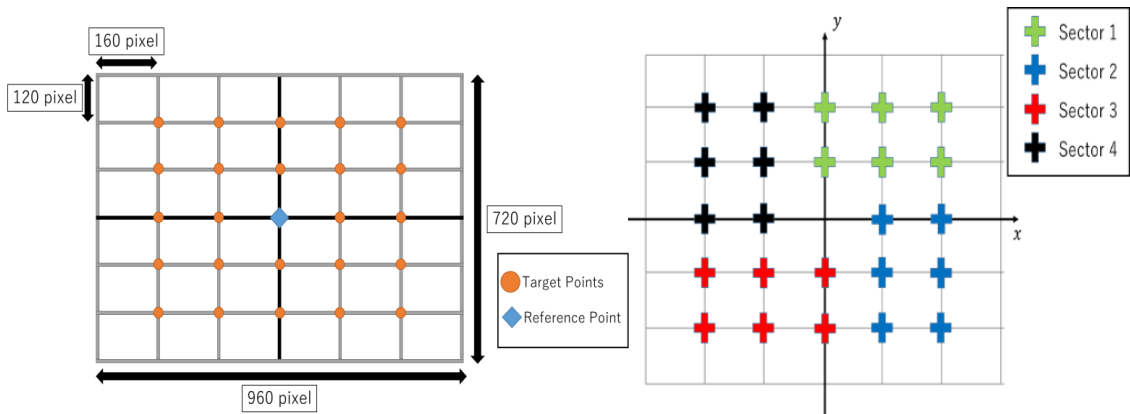


Figure 18. Eye Gaze Target Interface (Left) and Ideal Gaze Estimation (Right)

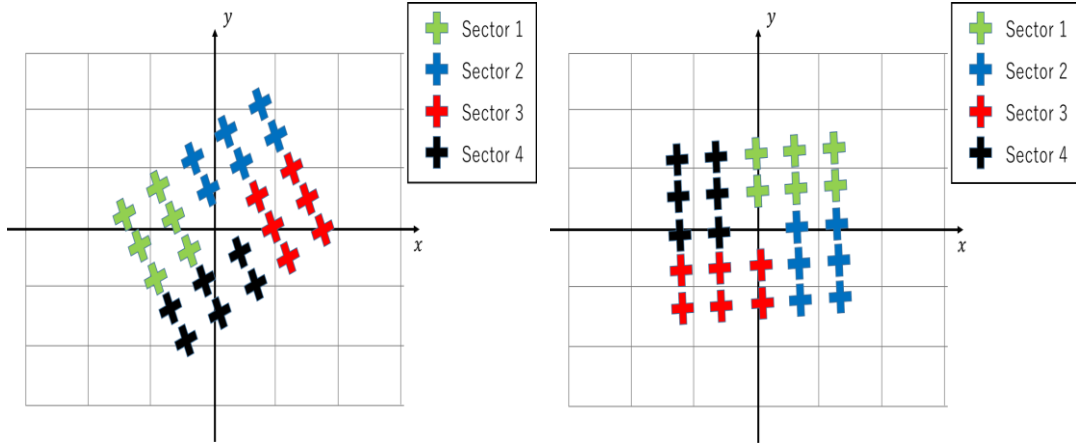


Figure 19. Cross-shaped electrode attachment(4-electrode) gaze estimation(left) and Plus-shaped electrode attachment(5-electrode) gaze estimation(right)

One of the techniques to solve the difference between gaze data and gaze target coordinates is by using a coordinate transformation technique. Previously, a 24-point gazing data calibration method was developed by Ilhamdi et al. [22] based on the cross-shaped electrode attachment to improve the gazing data. In this conventional method, the 24-point gazing data are spatially separated into quadrants. The data conversion is then implemented based on the quadrant.

However, we proposed a simpler computation using the affine transformation. Instead of separating the data, we propose a calibration method based on virtual origin coordinates. The conversion based on the proposed technique enables all gazing data to be calibrated simultaneously. Equations (6)–(9) shows the proposed homogeneous matrix for the affine transformation. The gazing data conversion (x', y') is determined using Equation (10).

$$\text{Homogeneous Matrix} = [\text{Dilatation}][\text{Rotation}][\text{Shear}][\text{Translation}] \quad (6)$$

$$= \begin{bmatrix} s_x(\cos \theta - m_2 \sin \theta) & s_x(m_1 \cos \theta - \sin \theta) & f_1 \\ s_y(\sin \theta + m_2 \cos \theta) & s_y(m_1 \sin \theta + \cos \theta) & f_2 \\ 0 & 0 & 1 \end{bmatrix} \quad (7)$$

$$f_1 = s_x(-T_x \cos \theta + T_x m_2 \sin \theta - T_y m_1 \cos \theta + T_y \sin \theta) \quad (8)$$

$$f_2 = s_y(-T_x \sin \theta - T_x m_2 \cos \theta - T_y m_1 \sin \theta - T_y \cos \theta) \quad (9)$$

$$\begin{bmatrix} x' \\ y' \\ 1 \end{bmatrix} = \text{Homogeneous Matrix} \begin{bmatrix} x \\ y \\ 1 \end{bmatrix} \quad (10)$$

There are four geometrical steps involved in the homogeneous matrix computation. Figure 20 illustrates each geometry process. The first step is the translation, where the imaginary center coordinate (T_x , T_y) is adjusted to the origin coordinates (0,0). The second step involves the shearing of the axes. The shear is to ensure that the axes of the captured gazing data are perpendicular to each other. The third step is to rotate the now perpendicular axes by an angle θ to match normal x-y plane. The final step is dilatation. Dilatation adjusted the gazing data to have a similar value with the gaze target pixel value. However, in this part, we separated the dilatation into four variables based on the line axis. The dilations are determined as:

- Dilatation s1 is for data located on the positive y-axis line;
- Dilatation s2 is for data located on the negative y-axis line;
- Dilatation s3 is for data located on the positive x-axis line;
- Dilatation s4 is for data located on the negative x-axis line.

Compared to the conventional method, the number and the order of the proposed geometrical steps are significantly different. The proposed method uses one less geometrical step than the conventional method. Besides, the total number of mathematical operation parameters required in the proposed method are nine: Two translation, two shear operations, one rotation, and four dilatation operations. Compared with the conventional method, which required seven operation parameters for each quadrant, giving twenty-eight operation parameters, this shows that the proposed method is simpler than the conventional method in terms of computational resources and time.

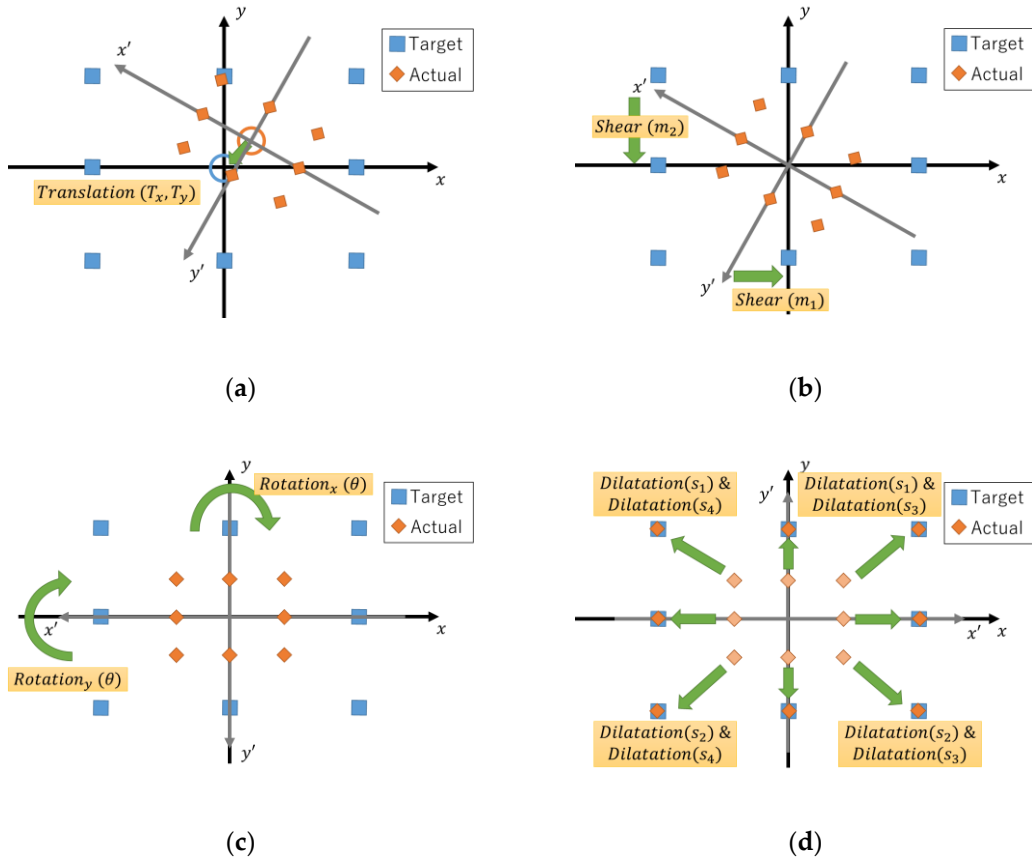


Figure 20. Proposed affine transformation geometry process. (a) Translation; (b) Shear; (c) Rotation; and (d) Dilatation.

2.6. Color-based Image Processing

Other than the calibration method for EOG gaze estimation, we proposed image processing as an alternative accuracy enhancement. Image processing offers autonomous identification for the position of gaze target. As examples, if there is an object used as the target, the image processing will identify the object's existence and compute the location. The location is then compared to gaze estimation to determine if the user is gazing on the object. As for the image processing method, we used a color-based image processing method. In this research, two colors have been chosen; red and blue colors.

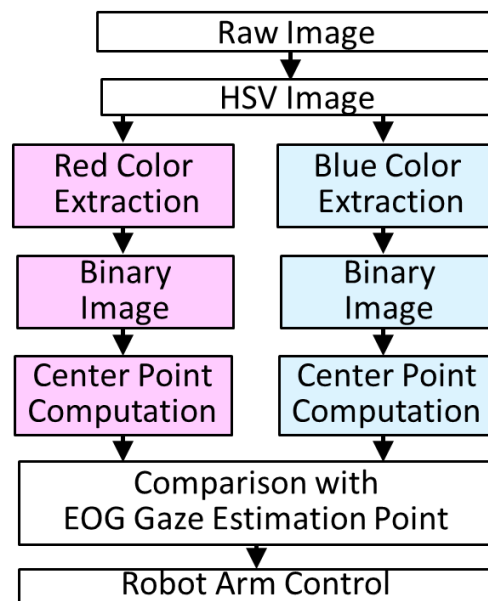


Figure 21. Red and blue object image processing process

Figure 21 shows the process of determining red and blue objects for image processing. Input or source videos from a camera are converted into that Red Green, and Blue(RGB) color based on a 3x8bit channel(24bit channel) raw image. To track a designated color in

an image, the image then converted into the color code of Hue, Saturation, and Value(HSV).

Using the HSV color code, we discriminated against the color red and blue from other colors. The discrimination then converted the image into a binary image where red and blue color is represented in white color and other colors in black color. Figure 21 shows the conversion red and blue objects image into a binary image.

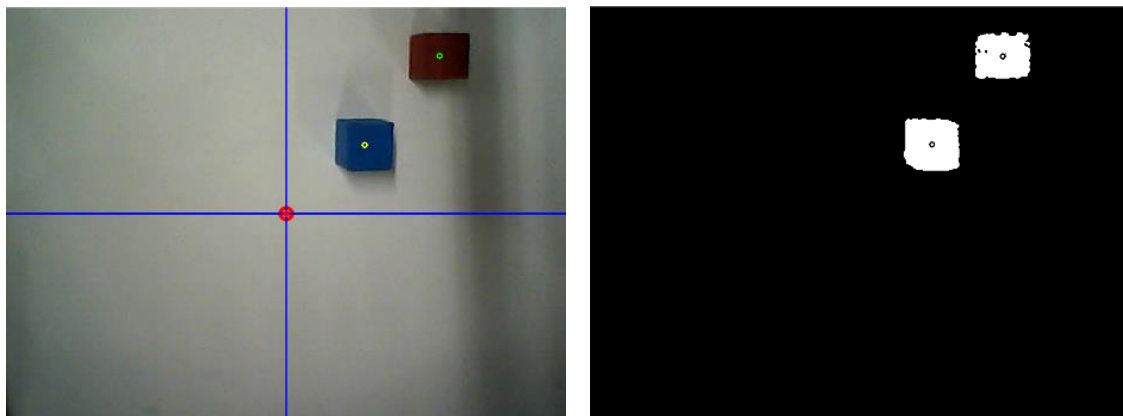


Figure 21. Red and blue raw image(left) and binary image(right)

From the binary image, we compute the center point of the objects by the Blob analysis technique. The center point of the objects then is used to assist the EOG gaze estimation by comparing the EOG gaze estimation coordinate with the object center point. The nearer the EOG gaze estimation to an object center point, the particular object is estimated to be selected by the test subject.

Chapter 3

EOG measurement stability (EOG Mask)

3.1. Background

Bio-signal control for welfare devices is one of the prospective technologies to enhance disabled people's quality of life (QoL). For that reason, we focus on electrooculography (EOG), which is the electrical potential generated by eye movement, and have been working on robot-arm control. So far, we have implemented an EOG-control scheme (Figure 22) and, as the next step, we try to enhance the convenience of the EOG interface.

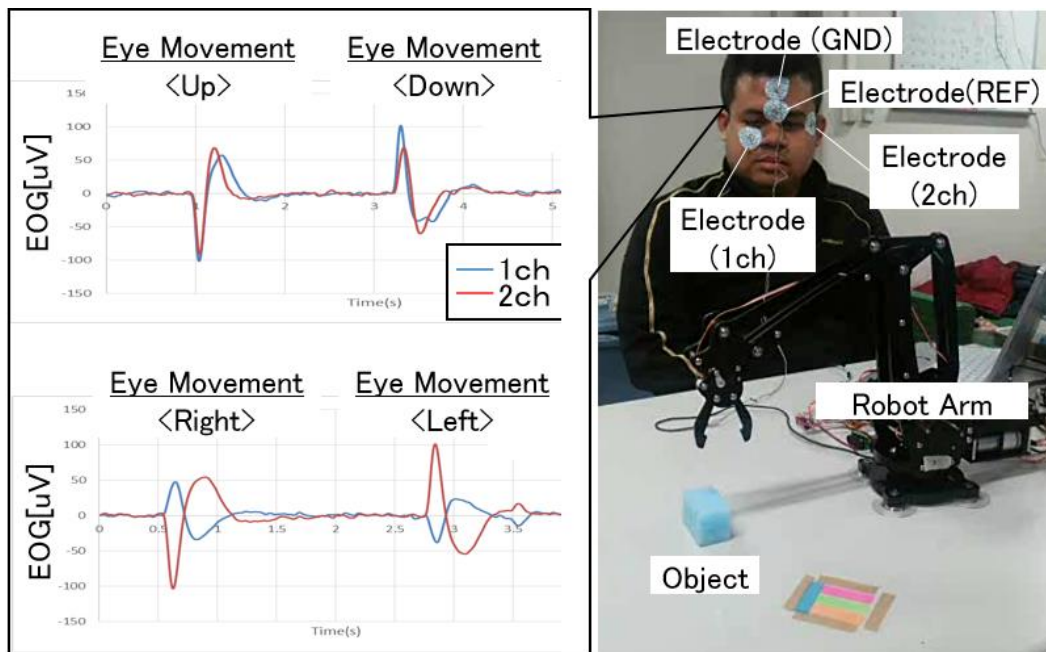


Figure 22. Conventional EOG based robot control method

The general EOG interface is made of 4-5 separated electrodes with long cables and those electrodes are applied for specific locations around the eye by hands. That is, the manual procedure inevitably makes location errors in millimeters or centimeters, and the system requires the calibration procedure for reducing those errors. Besides, the procedure is also time-consuming. Therefore, we propose to develop a custom-made EOG mask based on a 3D human face model with 3D scan and 3D printing techniques for easily, stably, and precisely locating those electrodes. Besides, we investigate the EOG signal stability with the proposed mask.

3.2. Experiment

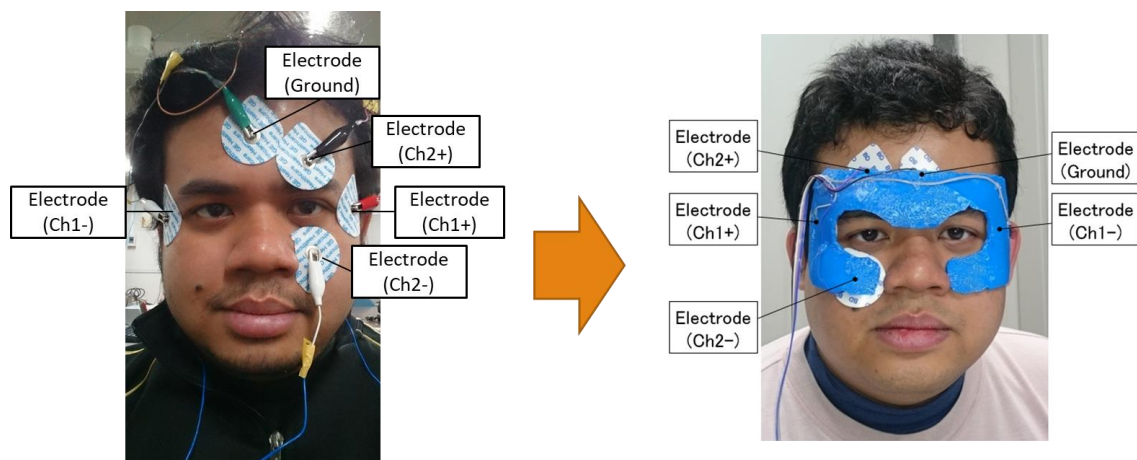


Figure 23. Conventional electrode attachment(left) and EOG mask method(right)

The plus-shaped electrode attachment method is used for the experiment. With the attachment method, two comparative placement methods; conventional manual hand electrode placement and proposed EOG mask methods are proposed for the experiment. Figure 23 shows the conventional attachment and EOG mask. The objective of the experiment is to investigate the stability of the EOG signals during performing 4-basics eye gaze; up, down, left and right.

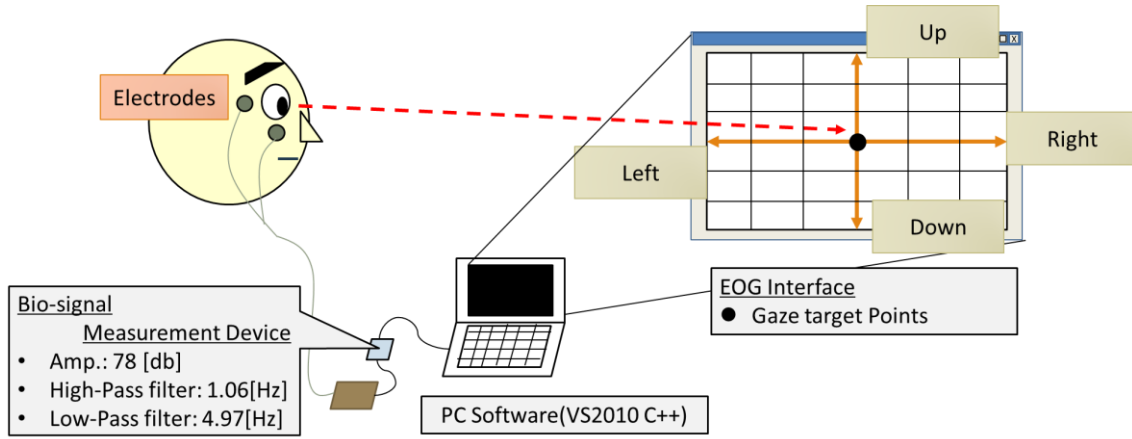


Figure 24 Experiment setup.

The test subject is instructed to perform eye gaze with the support Graphical User Interface(GUI) on a computer monitor. There are moving points to stimulate the 4-basic eye direction. The experiment setup is as shown in figure 24. To enhance the signal stability investigation, we proposed repetition in the electrode placement process to the experiment. Figure 25 illustrated the processes.

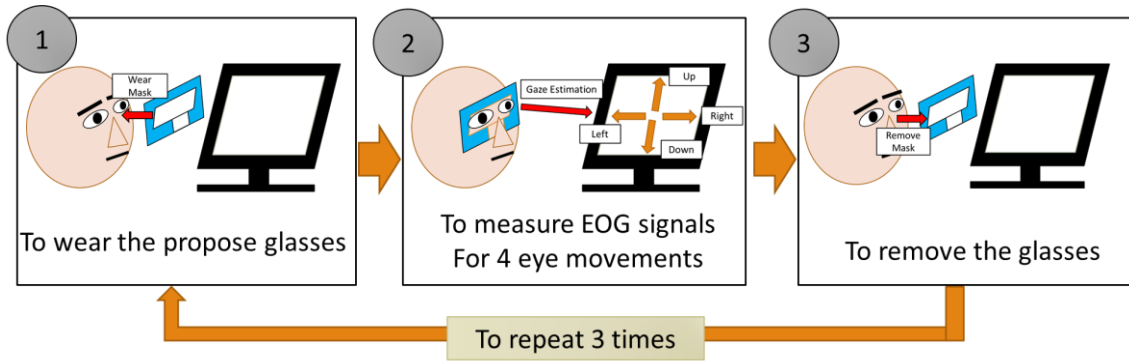


Figure 25 Proposed EOG mask experiment process.

At the start of the experiment, the test subject will attach or wear the electrode placement method. After the EOG signal for 4-basic directions is acquired, the test subject then removed the electrode placement. The process is repeated three times and the EOG signal stability is verified at the end.

3.2.1. Investigation on EOG signal stability for conventional electrode attachment and EOG mask

Figure 26 shows the results for the Ch1 EOG signal. All three EOG signals indicate almost the same characteristics in the pattern for both electrode placement methods. For the up and down eye gaze, we observed negligible EOG signal pattern. However, for the right and left eye gaze, there are similarities in the EOG signal pattern. Figure 27 shows the results for the Ch2 EOG signal. Similar results are observed for the signal characteristics. Based on the results, up and down eye gazes show similarities in the EOG signal pattern. For right and left eye gazes, the EOG signal shows a negligible signal pattern.

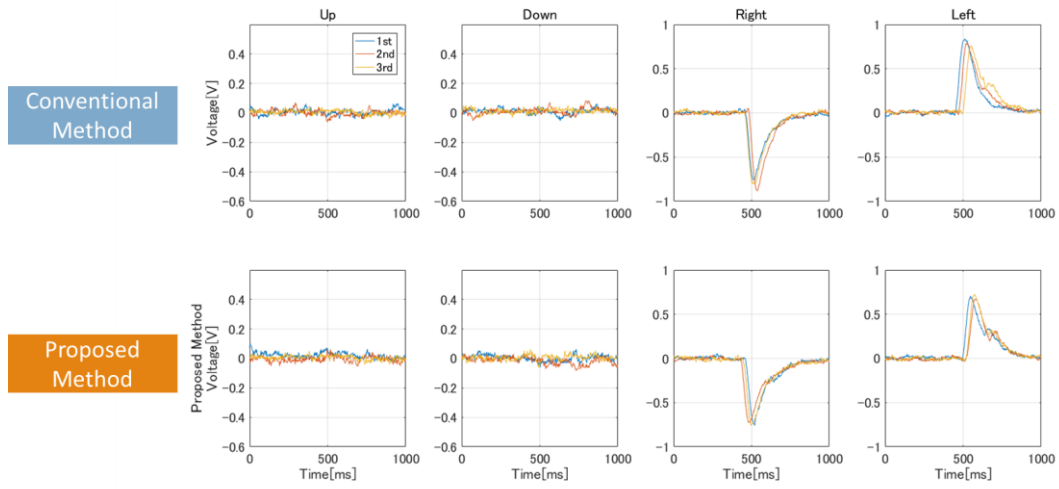


Figure 26. Ch1 EOG signal for 4-basic directions

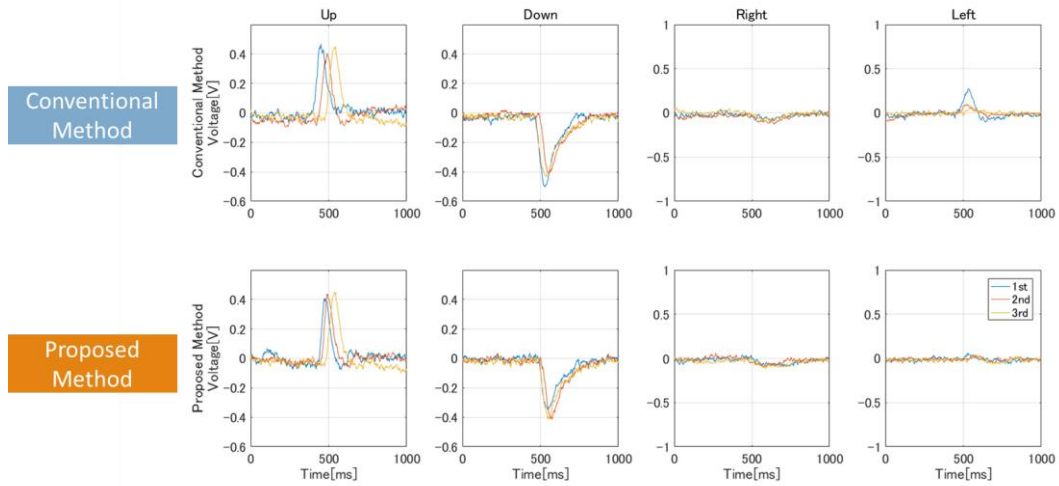


Figure 27. Ch2 EOG signal for 4-basic directions

Next, the EOG signal maximum amplitude is observed to discriminate for signal stability. Figure 28 shows the comparative signal amplitude for both placement methods. For the conventional method, the amplitude value shows higher inconsistency for all eye gaze directions. The EOG mask is also shown inconsistency, however, the disparity of amplitude value is minimal.

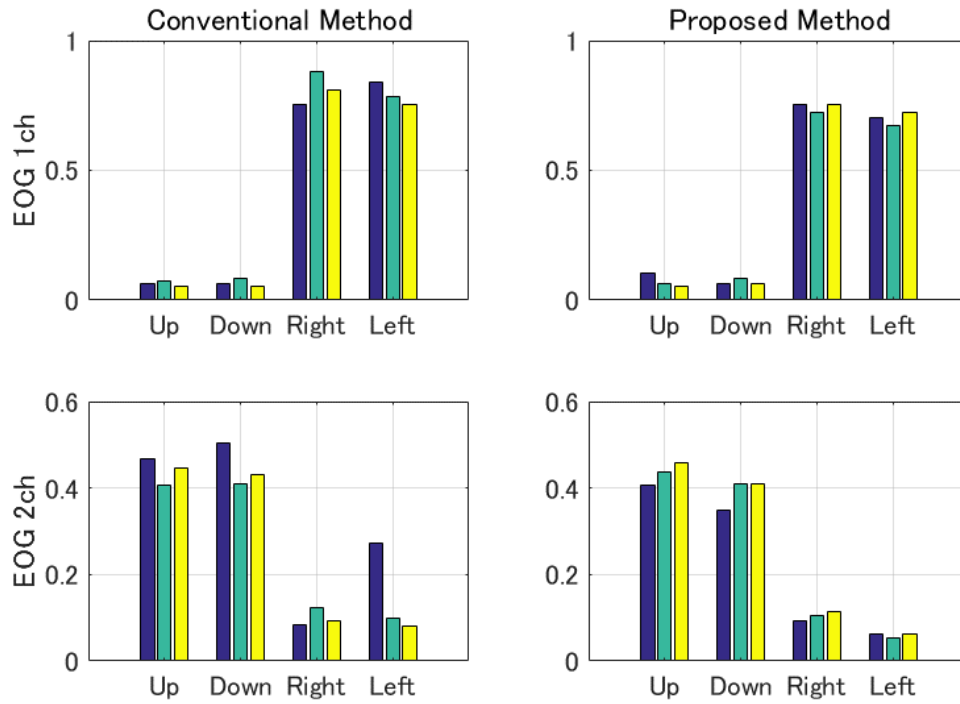


Figure 28. EOG signal amplitude value for 4-basic directions

Further analysis is conducted by observing the signal standard deviation value. Figure 29 shows the results of the standard deviation. From the 4-directions, the proposed EOG eye mask shows significantly better standard deviation results. Notably, using the right eye gaze result as an example, the deviation value for the conventional method is approximately 0.06 in compare 0.02 for the proposed method.

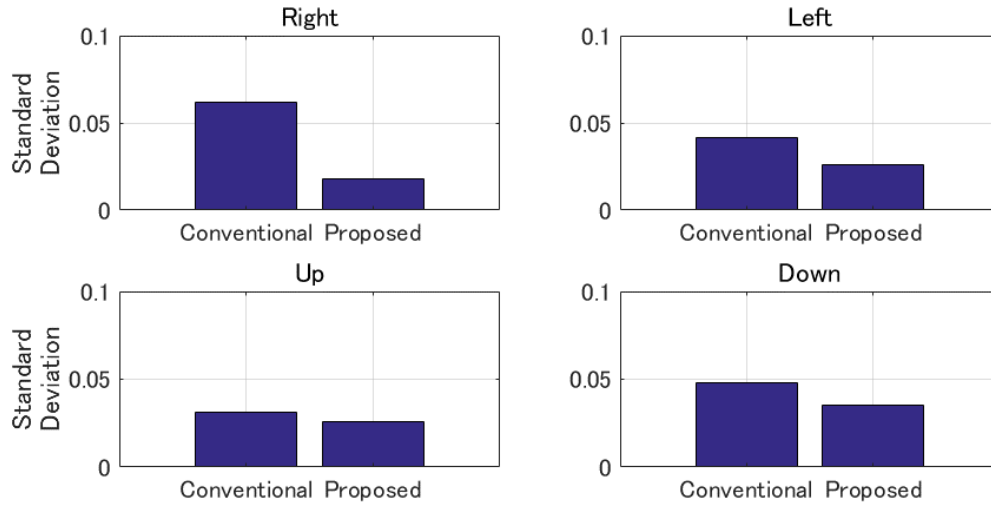


Figure 29. EOG signal amplitude value for 4-basic directions

3.3. Discussion

In this paper, we proposed a custom-made EOG mask for providing stable EOG measurements. The mask manufacturing process is to acquire a 3D face model with a 3D scanner and to modify the model to the design of the mask, and to build the mask with a 3D printer. An investigation on EOG signal stability is conducted to compare the conventional manual hand electrode placement and the proposed method. The test subject is required to perform 4-directions eye gaze with the repetition of placing and removing electrode placement method 3 times.

Based on the result, both methods show similarities in signal patterns. As for the signal maximum amplitude value, we observed a minimal inconsistency for the EOG mask. Further signal analysis is done by standard deviation computation. The EOG mask shows significantly better standard deviation results. From the overall analysis, we concluded that the EOG mask not only is simple and quick for EOG signal measurement, the signal is also more stable than the conventional electrode placement method.

Chapter 4

Calibration method for AC-EOG Gaze Estimation

4.1. Background

The direct human gaze is an indicator of interest. Thus, eye tracking has become one of the most prospective technologies in recent years. There are two types of major eye-tracking systems: One is to record pupil positions with infrared cameras [26-27], and the other is to record electro-oculo-graphic (EOG) signals with a biological signal measurement device [1]. The camera-based system requires the user to wear camera built-in glasses [28-29] or to fix their head position to achieve the stable capturing of their pupils. This imposes physical burdens, such as heaviness and motion and visual restriction on the user [30-31].

Besides, this method is slightly difficult for users who wear glasses and contact lenses due to reflection from the lenses, which makes the system unable to detect the pupils stably. Whereas the EOG-based system is characterized by gaze point precision, which is less than that of the camera-based system, the EOG is more robust in determining gaze direction [32-33]. In the EOG, data acquisition is achieved by attaching a few disposable electrodes around their eye of the subject and has the advantage of being less burdensome to the eyes in the measurement of the eye movement.

There are two types of EOG analysis methods: Direct-current-EOG (DC-EOG) and alternating-current-EOG (AC-EOG). DC-EOG signals are almost raw EOG signals, and the amplitudes are directly related to the eye movement [3]. DC-EOG has a disadvantage in that the resulting signals are easily influenced by human movement, and motion restriction is required to ensure precise acquisition [4-5]. On the other hand, AC-EOG is a DC-EOG which has been augmented with a band-pass filtered DC-EOG and is strongly against human movements. The signals are characterized to automatically adjust to zero so that the amount of eye movement is calculated with the signal integral [5].

However, the AC-EOG-based gaze estimation method requires calibration to the signal before implementation. The user is required to gaze at several target points, and each signal is used for determining the conversion parameters from eye moment and gaze estimation at the calibration phase. The calibration is the most important factor since it adjusts individual differences caused by electrode attachment, such as plus-shaped five-electrode arrangement and cross-shaped four-electrode arrangement.

Ilhamdi et al. [8-10] studied the application of AC-EOG gaze estimation for robot control. Four electrodes were attached around the user's eyes in the cross-shaped arrangement and the calibration was made using affine transformation based on the 24-point-group gaze target. The method was well-converted from two EOG signals to a gaze point on the gaze target. However, the transformation was performed for each quadrant, rather than simultaneously. Then, the quadrant method assumed all the data in one set in space are of the same polarity. However, the significant rotation could disrupt the data polarity. Thus, each quadrant had different characteristics, and data polarity disruption by rotation led to low accuracy.

In this chapter, we focused on improving the accuracy of AC-EOG gaze estimation by proposing an alternative 24-gaze-point affine transformation calibration method. A virtual origin was computed which, together with 24 gaze points, formed 25 gaze points which are affine transformed. In this work, we analyzed and compared the accuracy of the calibration technique employed earlier, proposed by Ilhamdi, and the technique proposed for the research. We applied the proposed method to two traditional AC-EOG signal measurements (i.e., cross-shaped electrode arrangement and plus-shaped electrode arrangement) and demonstrated its superiority in terms of accuracy.

4.2. Experiment

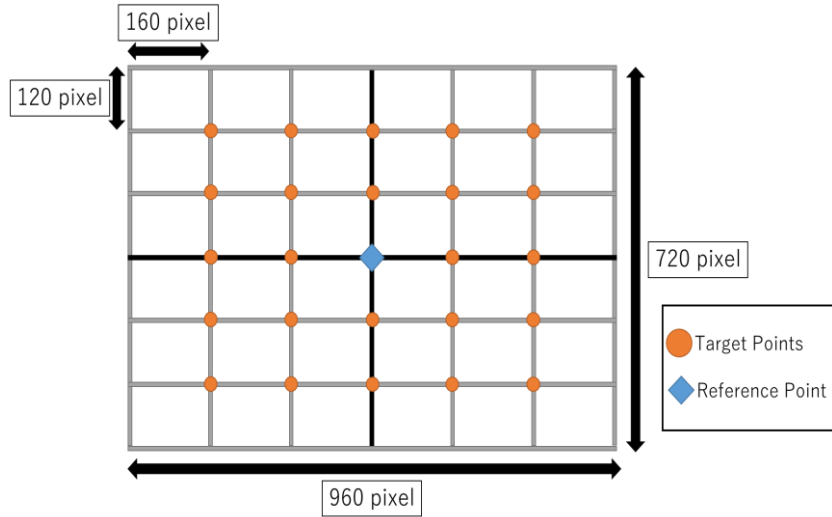


Figure 30. 24-point eye gaze target

The objective of the research is to investigate the accuracy of EOG gazing data with gaze target points. A 24-point targets based on a Graphical User Interface(GUI) program are built as the target for eye gaze. Figure 30 shows the interface for the experiment. Target points are represented in pixel value and reference points served as target points center coordinates (0,0). The relationship between EOG and eye gazing is determined by analyzing the EOG data and compared with the target pixel value.

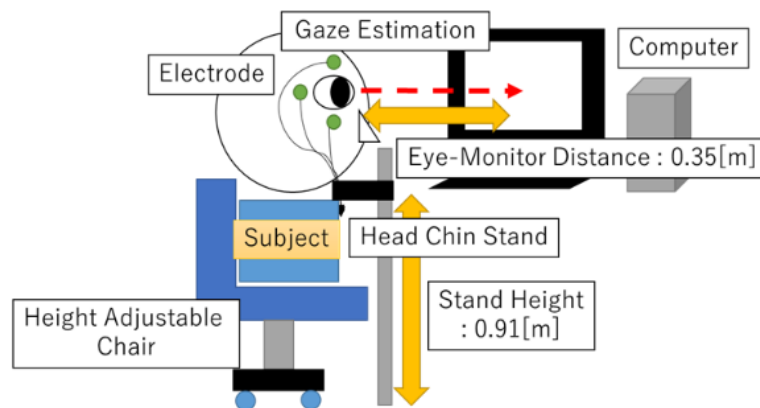


Figure 31. Experiment setup

Ten test subjects are requested to perform the experiment. With the head fixed on a stand, the test subject is instructed to perform eye gaze between the reference point and target points. A distance of 35 cm between the test subject head and the computer screen is maintained to calculate of angle error between the eye and gaze target. Figure 31 illustrated the setup for the experiment.

4.3.1. Investigation on Coordinate Transformation for Cross-shaped electrode attachment method

A comparative investigation experiment was conducted to compare the accuracy of the conventional cross-shaped electrode attachment method conversion method with the proposed method. Four simulation patterns of 24-point gazing data were proposed for the experiment. The patterns were used to test each computation in affine transformation homogeneous matrix: Dilatation, rotation, shear, and translation. To investigate the accuracy, the pixel distance error was used as an indicator, where the lower the distance error value, the higher the accuracy. Figure 32 shows the simulation patterns used in the experiment. The specification for each pattern computation objectives is as such:

- 1) Pattern (a) is to test dilatation and rotation;
- 2) Pattern (b) is to test dilatation, rotation, and translation;
- 3) Pattern (c) is to test dilatation, rotation, and shear;
- 4) Pattern (d) is to test dilatation, rotation, shear, and translation.

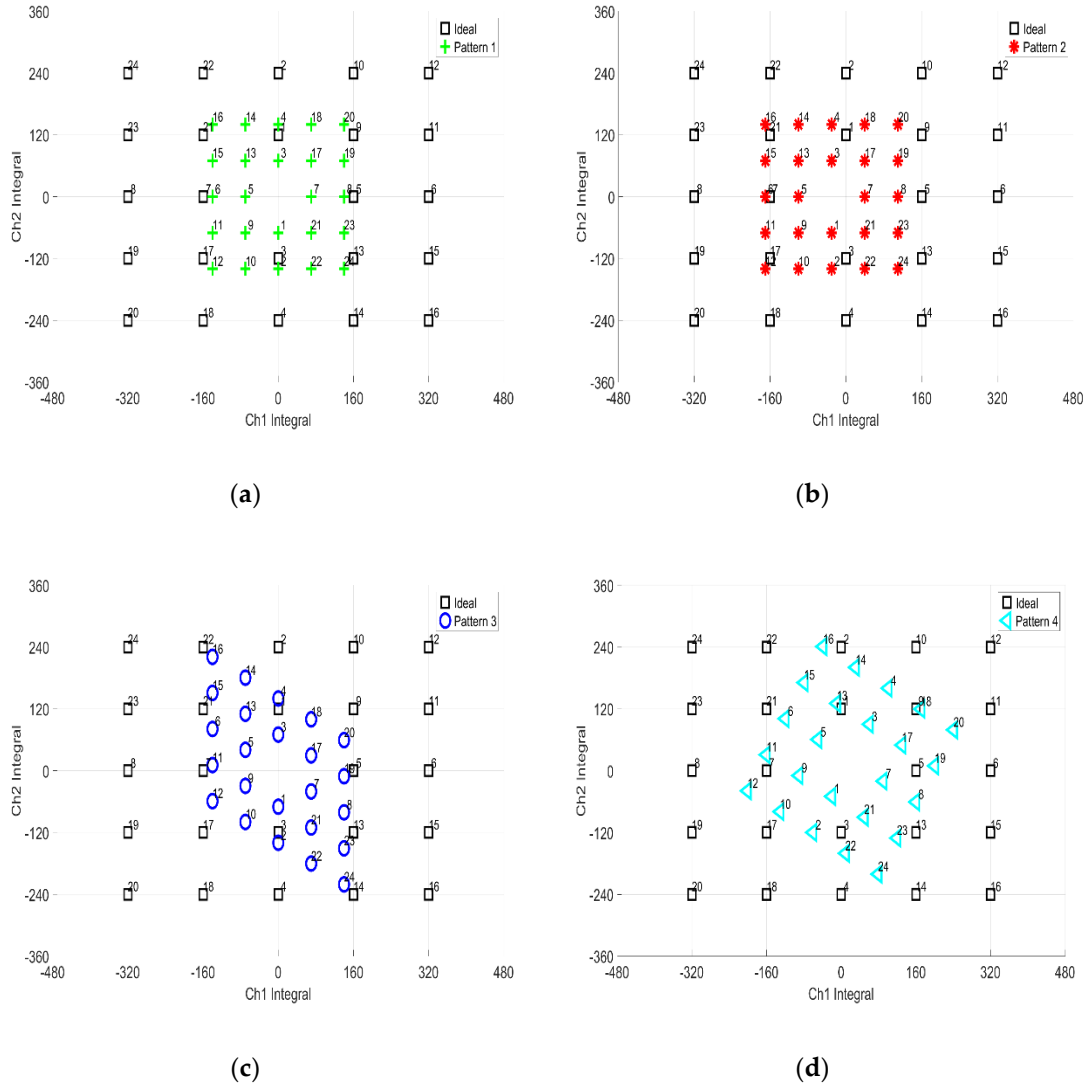


Figure 32. Simulation patterns for 24-point computation: (a) Dilatation and rotation; (b) Dilatation, rotation and translation; (c) Dilatation, rotation and shear; (d) Dilatation, rotation, shear and translation.

In the pattern simulation graph, the desired result(ideal points) is shown as the black square. The simulation patterns which are represented in plus or asterisk points are based on the conversion of ideal points to be smaller or rotated. The simulation objective is to use the calibration methods to correct the simulation patterns into ideal points again.

Figure 33 shows the computation results. Based on the results, the proposed method performed better in calibrating the simulated gazing data relative to the conventional technique. From the four patterns, the average pixel distance error for the x and y pixel was negligibly small for the proposed method. This meant that no pixel distance errors were observed for the proposed method. In contrast, the average pixel distance error for x pixel was 11 ± 3 pixel and for y pixel, the error was 5 ± 2 pixels for the conventional method. From the results, the proposed virtual origin coordinate conversion method is significantly better than the conventional method.

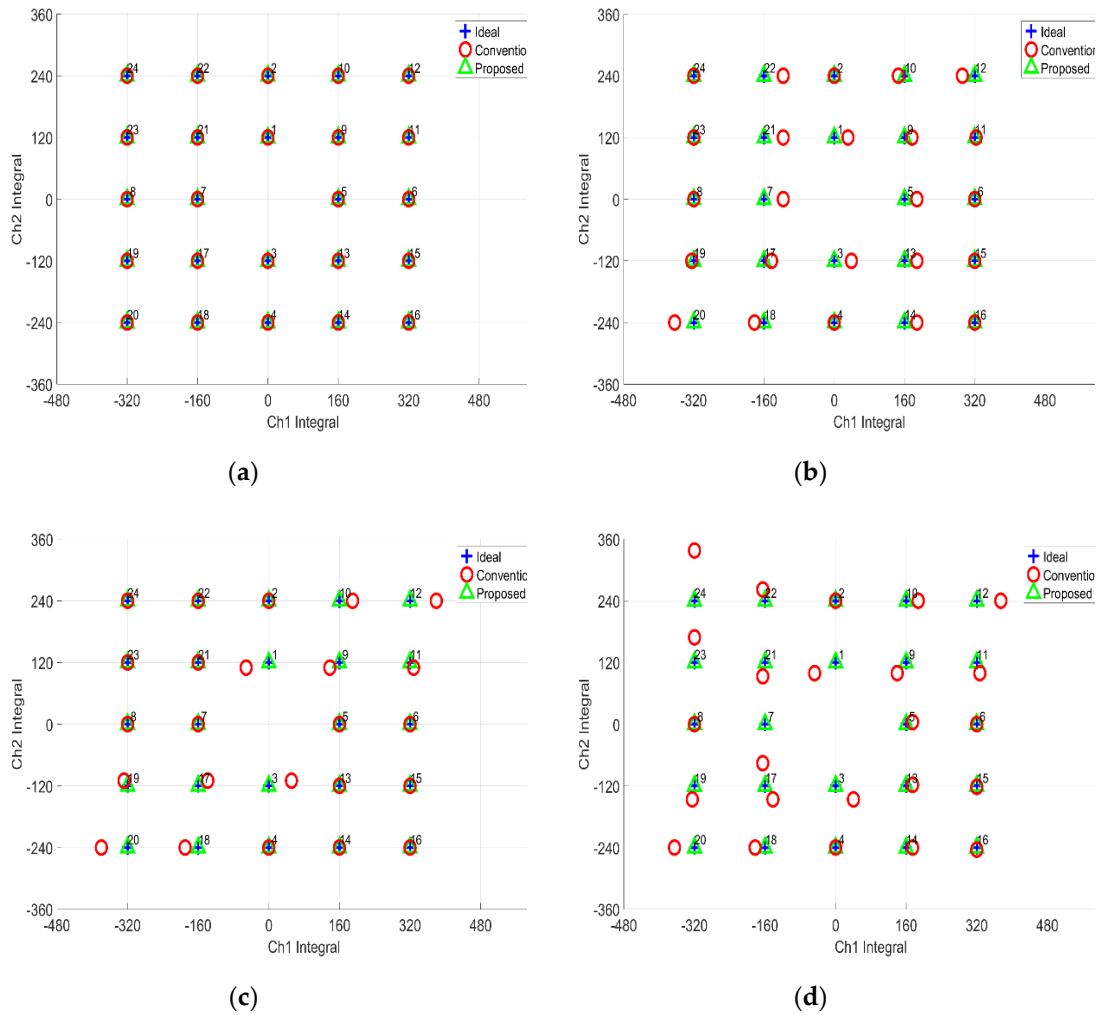
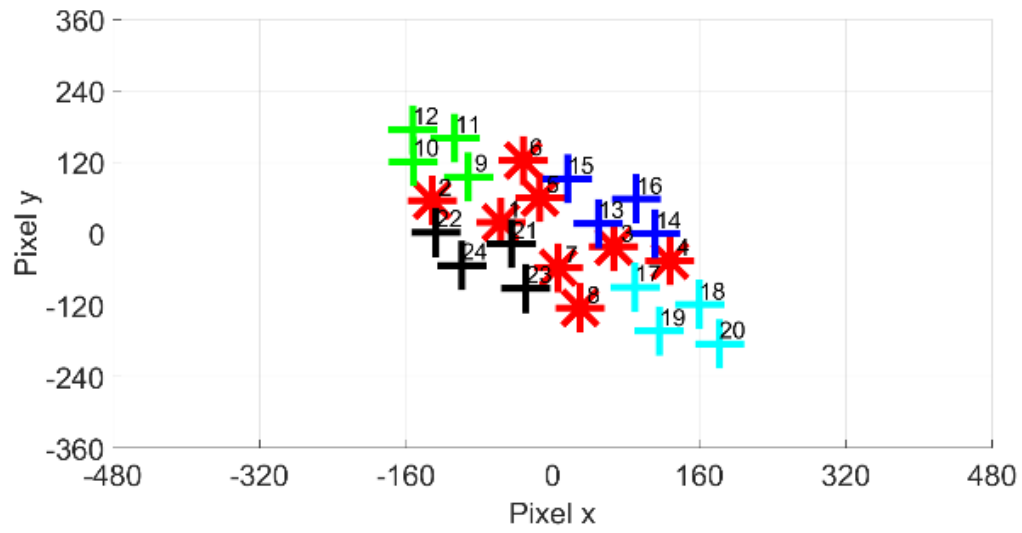


Figure 33. Simulation results for 24-point computation: (a) Dilatation and rotation; (b) Dilatation, rotation and translation; (c) Dilatation, rotation and shear; (d) Dilatation, rotation, shear and translation.

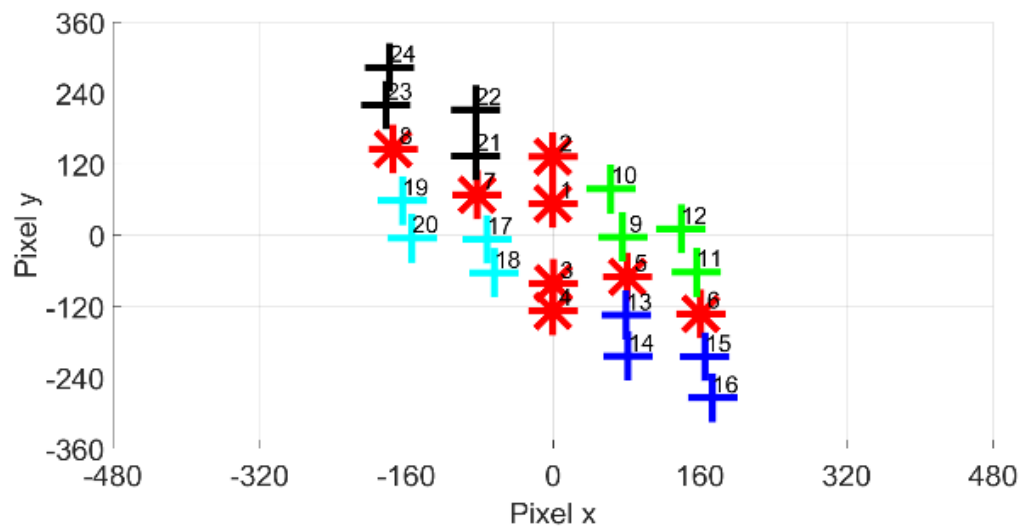
The errors observed for the conventional method are attributed to quadrant separation-based computation. The quadrant method restricts the view on the calibration into a small set of data. The data near the x and y-axis are adversely affecting the computation. The quadrant method assumed all the data in one set in space are of the same polarity. If the rotation is significant, the data polarity is disrupted. The borderline data polarity, when used for computation, became inconsistent and then affected the accuracy of the calculations. In the proposed method, however, the 24-point gazing data are calibrated simultaneously, making the method not only simpler but also accurate when it comes to computation.

3.3.2. Investigation on Cross-shaped electrode attachment and Plus-shaped electrode attachment to the AC-EOG Accuracy

In this section, we performed a comparative investigation of the accuracy of the proposed method using EOG gazing data. Ten samples of 24-point gazing data were taken for both electrode attachment methods. We determined the accuracy based on gaze angle error. The lower the angle degree, the more accurate the gazing data. Figure 34 illustrates the original EOG gazing data.



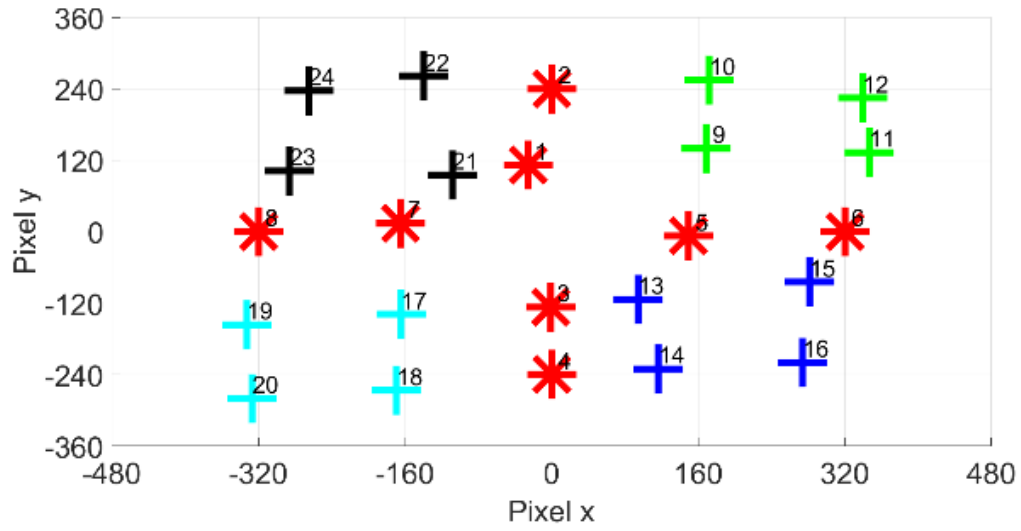
(a)



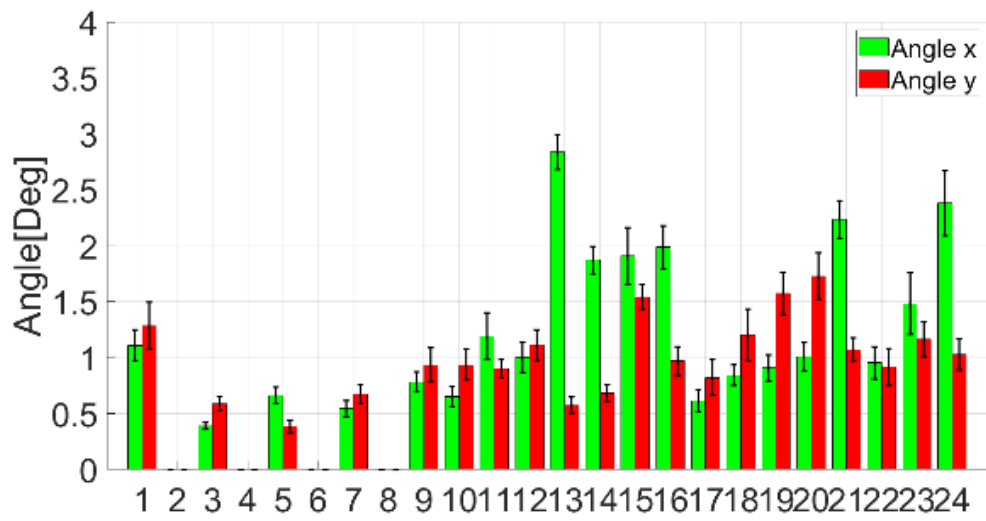
(b)

Figure 34. Original EOG gazing data: (a) Cross-shaped electrode attachment; (b) Plus-shaped electrode attachment.

Figure 35 shows the result of the cross-shaped electrode attachment. Compared to the original EOG gazing data, the accuracy is greatly improved. The calibrated 24-point gazing data achieved compelling similarity with gaze targets. Based on the bar chart, most of the x and y error angle for each point is less than 2° . On the other hand, Figure 36 shows the results of the plus-shaped electrode attachment. Likewise, compared to the original EOG gazing data, the accuracy is also greatly improved. The gaze error angle observed from bar chart shows that the x and y angle error is less than 2° .

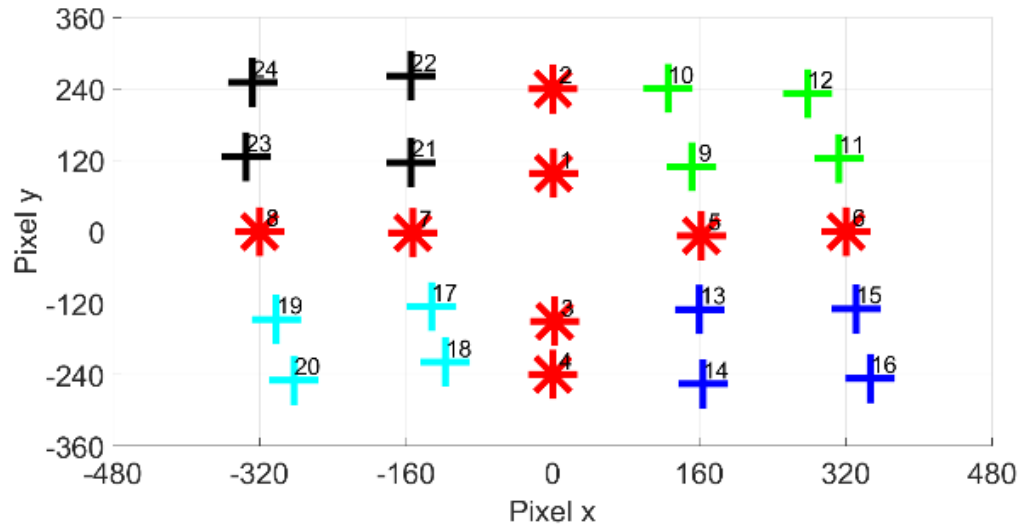


(a)

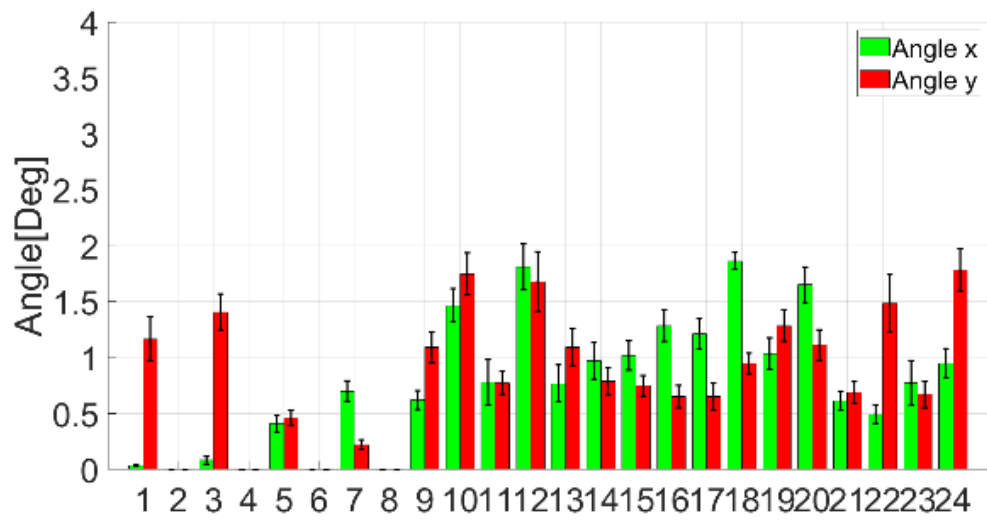


(b)

Figure 35. Cross-shaped electrode attachment conversion results: (a) Calibrated 24-point gazing data; (b) Gaze angle error for each point.



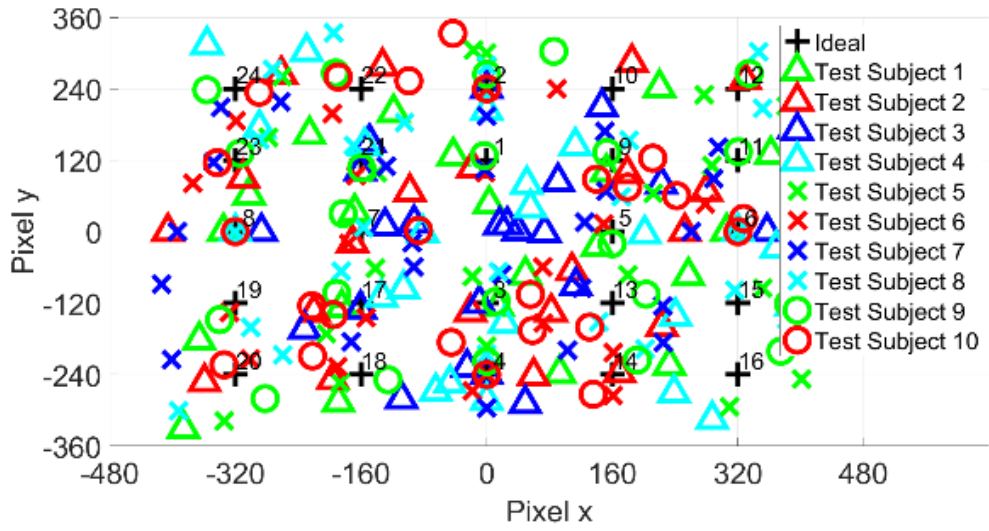
(a)



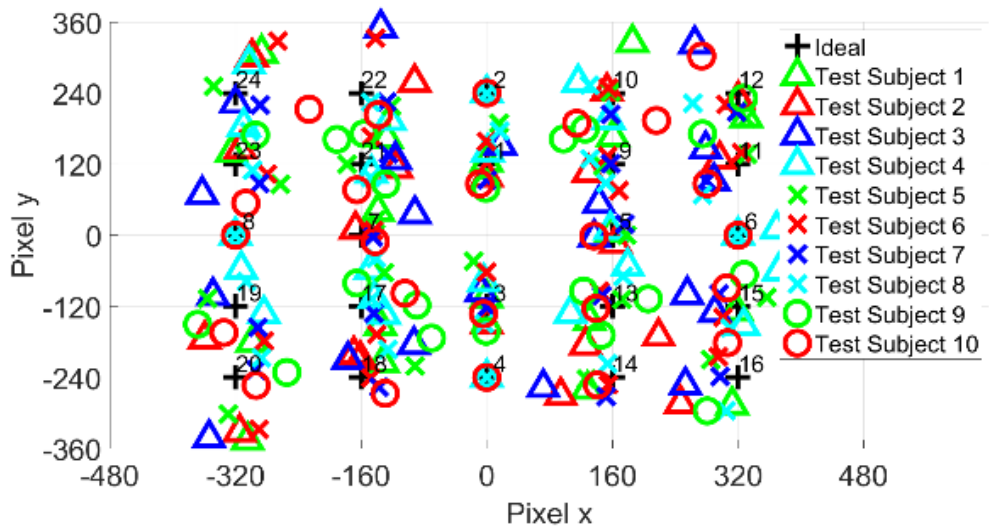
(b)

Figure 36. Plus-shaped electrode attachment conversion results: (a) Calibrated 24-point gazing data; (b) Gaze angle error for each point.

The next step in the experiment is to obtain EOG gazing data from 10 test subjects. The test subjects are to strengthen the investigation on the accuracy of the proposed method. However, instead of observing the gaze angle error on a point-to-point basis, the average for 24-point is calculated. The results for gazing data are shown in Figure 37. The test subjects' average gaze angle error results are shown in Figure 38, Table 7, and Table 8. The ten test subjects' average for the cross-shaped electrode attachment is $x=2.27^{\circ}\pm0.46^{\circ}$ and $y=1.83^{\circ}\pm0.34^{\circ}$. In comparison, the average for the plus-shaped electrode attachment is $x=0.94^{\circ}\pm0.19^{\circ}$ and $y=1.48^{\circ}\pm0.27^{\circ}$. From the gaze angle error result, both electrode methods shows gaze angle errors. However, the plus-shaped electrode attachment method shows a relatively small x and y gaze angle error compared to the cross-shaped electrode attachment.

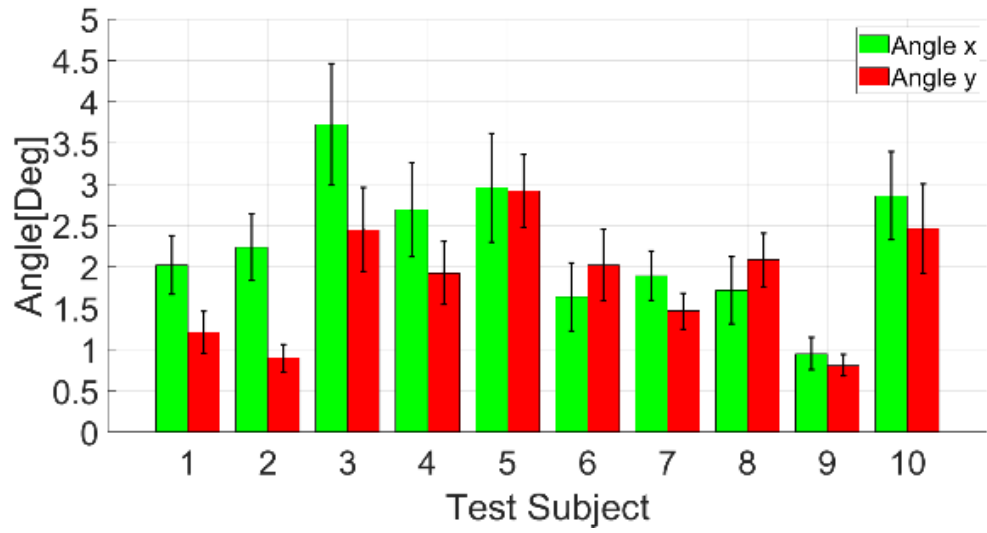


(a)

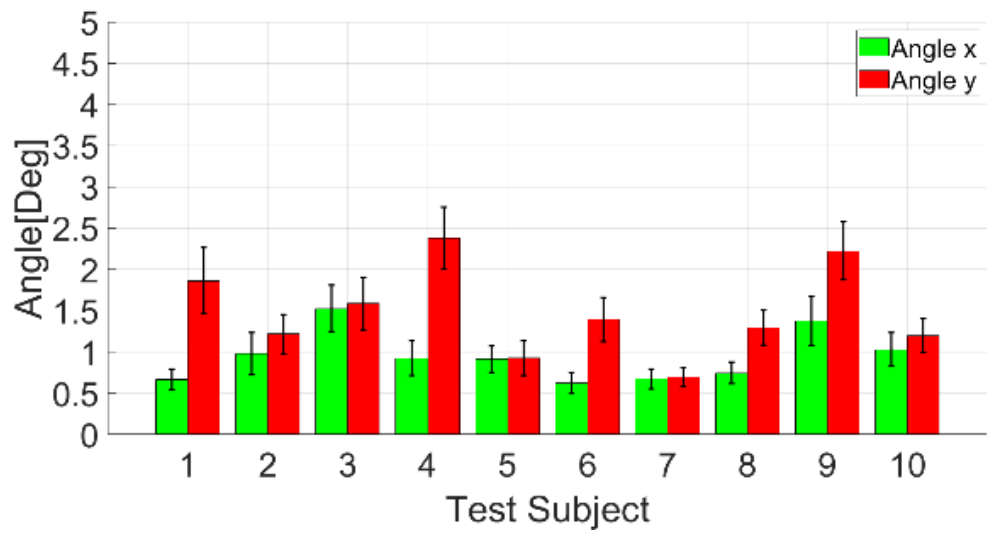


(b)

Figure 37. Twenty-four-point gazing data for 10 test subjects (a) Cross-shaped electrode attachment; (b) Plus-shaped electrode attachment.



(a)



(b)

Figure 38. Average 24-point gaze angle error for 10 test subjects: (a) Cross-shaped electrode attachment; (b) Plus-shaped electrode attachment.

Table 7. Cross-shaped electrode attachment average 24-point gaze angle error for 10 test subjects.

Subject	Ave. Angle x (θ°)	Ave. Angle y (θ°)	x SD (σ_x°)	y SD (σ_y°)
1	2.0205	1.2098	0.3555	0.2517
2	2.2390	0.8978	0.4006	0.1682
3	3.7267	2.4537	0.7384	0.5082
4	2.6903	1.9262	0.5695	0.3820
5	2.9605	2.9202	0.6591	0.4417
6	1.6390	2.0228	0.4146	0.4356
7	1.8961	1.4659	0.2978	0.2190
8	1.7187	2.0854	0.4073	0.3257
9	0.9506	0.8094	0.1957	0.1324
10	2.8613	2.4653	0.5350	0.5427
Average	2.2703	1.8256	0.4574	0.3407

Table 8. Plus-shaped electrode attachment average 24-point gaze angle error for 10 test subjects.

Subject	Ave. Angle x (θ°)	Ave. Angle y (θ°)	x SD (σ_x°)	y SD (σ_y°)
1	0.6627	1.8633	0.1280	0.4032
2	0.9768	1.2166	0.2554	0.2388
3	1.5283	1.5873	0.2783	0.3169
4	0.9221	2.3825	0.2106	0.3763
5	0.9128	0.9252	0.1598	0.2105
6	0.6242	1.3943	0.1284	0.2691
7	0.6691	0.6944	0.1211	0.1133
8	0.7453	1.2921	0.1303	0.2095
9	1.3774	2.2247	0.2976	0.3514
10	1.0307	1.1971	0.2007	0.2041
Average	0.9449	1.4777	0.1910	0.2693

From the experiment, the proposed method proved to increase the accuracy of EOG gazing data for two different electrode attachment methods. However, in terms of the simplicity of the conversion method, the plus-shaped electrode attachment offered simpler computation than the cross-shaped electrode attachment method. The rotation for plus-shaped electrode attachment is negligible. Thus, the cross-shaped electrode attachment has nine operation parameters for affine transformation, but we had eight operation parameters for the plus-shaped electrode attachment.

3.4. Discussion

The objective of the research was to enhance the accuracy of the EOG gaze estimation method. The AC-EOG signal method was used to estimate the eyeball movement and the gaze position was determined by converting the captured signals. In conventional research, the affine transformation was introduced as a calibration method for 24-point gazing data from the two AC-EOG signals, corresponding to vertical and horizontal eyeball movements using the cross-shaped electrode attachment method. However, the transformation was not applied for all the 24-point gazing data but was instead applied for four spatially separated data (quadrant method). The quadrant method was also easily influenced by data rotation. The quadrant method assumed all the data in one set in space are of the same polarity, however, the significant rotation could disrupt the data polarity. The influence of data rotation was not fully investigated, as one electrode attachment method (cross-shaped four-electrode attachment) was used. Then, in terms of the computational complexity of the quadrant method, seven variables were computed in each quadrant, where each quadrant produced a different value. In this paper, we proposed

the conversion method for 24-point gazing data simultaneously and assumed a virtual origin (i.e., 25th point) on gaze coordinates with 24-point gazing data and applied an affine transformation to 24-point gazing data. Two experiments were conducted as a comparative investigation for the conventional and proposed methods. The first experiment was an accuracy investigation between the proposed method and conventional computation. Four simulation patterns, based on 24-point gazing data, were used, and the accuracy was determined by the pixel distance error. The result shows that the proposed method achieved negligible error in gazing data conversion. The second experiment was to determine the accuracy of the proposed method using EOG gazing data. Ten test subjects were used to performed 24-point gaze targets with two different electrode attachment methods. The average angle error for the cross-shaped electrode attachment was $x=2.27^{\circ}\pm0.46^{\circ}$ and $y=1.83^{\circ}\pm0.34^{\circ}$. On the other hand, the plus-shaped electrode attachment had an error of $x=0.94^{\circ}\pm0.19^{\circ}$ and $y=1.48^{\circ}\pm0.27^{\circ}$. The results show that there was a minimal error using the proposed method, and the two electrode attachment methods resulted in almost identical performances. From the experiments, we conclude that the proposed method was simpler and more accurate in EOG gaze estimation than the conventional method.

Chapter 5

Robot Control based on EOG Gaze Direction and Gaze Estimation

5.1. Background

Physically disabled people are commonly associated with low Quality of life(QoL). Those who are suffering from Amyotrophic lateral sclerosis(ALS) or Motor Neuron Disease (MND) are unable to manage their daily life. They constantly need other people to support. The advancement of robotic which has already improving ordinary people's life could provide the necessary assistance.

However, interaction difficulties existed between the physically disabled and the robot. The common control is based on hand or leg manipulation. Thus, we believe that one of the best non-physical interaction is by using bio-signal based control. For this, we are focusing on Electrooculography (EOG)[1]. The EOG is a method of detecting the electric potential between cornea and retina. As the eye movements, there changes in potential value[2].

There are two methods of eye gaze EOG control; gaze direction and gaze estimation. The gaze direction is a method of discriminating the signal to determine the direction of eye movement. The common EOG studies use gaze direction as control methods such as

PC cursor&click operation [13-19], robot arm operation[20-23], and electrical wheelchair operation[24-25] using this method. The gaze direction discrimination requires a simple EOG analysis method, but it has limited control capability. The maximum eye movement directions could be discriminated is 8-direction.

On the other hand, gaze estimation is a method discriminating against the EOG signal for eye gazing position. Ilhamdi et al. [8-10] studied the application of gaze estimation for robot control. In his research, he used a signal integral computation to discriminate the eye gazing position on the computer monitor. However, a calibration method comprising affine transformation is used to improve the accuracy of gaze estimation. As a result, he able to manipulate the robot arm to any location of his eye gazing. This shows that gaze estimation has great control capability but requires a more complex EOG analysis.

Other than the EOG as a control method, EMG which is a bio-signal from muscle is useful to simplify and increase the control input. For the EMG to be implemented together with EOG, the EMG need to be derived from the area on the face which near to the eyes. One of the possible EMG input is by the mouth muscle when the biting motion is performed. The EMG is useful as an additional control to stimulate grasp or release.

In this chapter, we are determining the EOG gaze methods is the best method for robot control. A 3D robot system has been proposed for the experiment. Using gaze direction or gaze estimation control method, an object displacement task is proposed. For the gaze estimation, we proposed a color-based image processing instead of an affine transformation calibration method to improve the gaze estimation accuracy. Then, the EMG from biting motion is proposed as an additional control to assist the object gripping. The time uses to complete the task is used as the basis of the performance investigation.

5.2. The proposed robot control system

5.2.1. Experiment setup

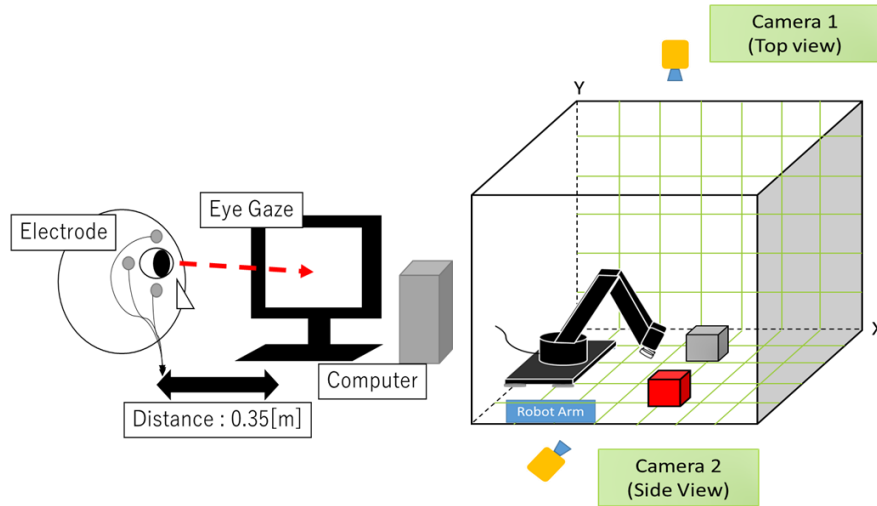


Figure 39. Proposed robot system setup

Figure 39 shows the proposed robot control system to compare EOG gaze methods. The objective is to determine which gaze methods; gaze direction or gaze estimation is the best for robot control. The gaze direction is a method analyzing the eyeball directional movement and gaze estimation is a method determining the eye gazing point. However, the gaze method alone is inadequate for certain control. For that, the robot system is to control the robot using EOG gaze direction or gaze estimation with supportive control from eye blink and EMG bite to enable the robot control for displacing a target object to a designated target position.

Then, an additional investigation is conducted to determine the robot efficiency corresponding to gaze distance error to object center point(gaze estimation control) and robot movement (gaze direction control). For the gaze direction, each direction will manipulate the robot arm with 2[cm] or 3[cm] movement. For gaze estimation, the gaze error distances of 2[cm] or 3[cm] to compare with the object center coordinate to determine object selection. The selection then guides the robot arm movement. The time completion for the object displacement is used as an indicator in which distance is the best and then compared to determine which gaze method performs better.

Five test subjects (age range from 20 to 40 years old) are invited for the experiment. The test subjects are instructed to perform the object displacement with the help of a computer monitor screen. The test subjects are distanced from the monitor at the approximation of 0.35[m]. Two cameras have been used to simulate a 3D robot workspace. One of the cameras shows the top view which corresponding to the x and y-axis of the robot movement. The other shows the side view which corresponding to the y and z-axis robot movement.

Two target objects have been chosen for the experiment; red and blue cube target objects. The colors are specified as we purpose to assist the EOG gaze estimation with color-based image processing. Image processing is used to determine the object center coordinate which used to compare with eye gaze estimation. The comparison is used to determine the error distance which will be used to find appropriate error distance for object selection. Figures 39 and 40 show the top and side view of the camera image with the information of the initial robot arm position, red and blue target objects and yellow area as target displacement position.

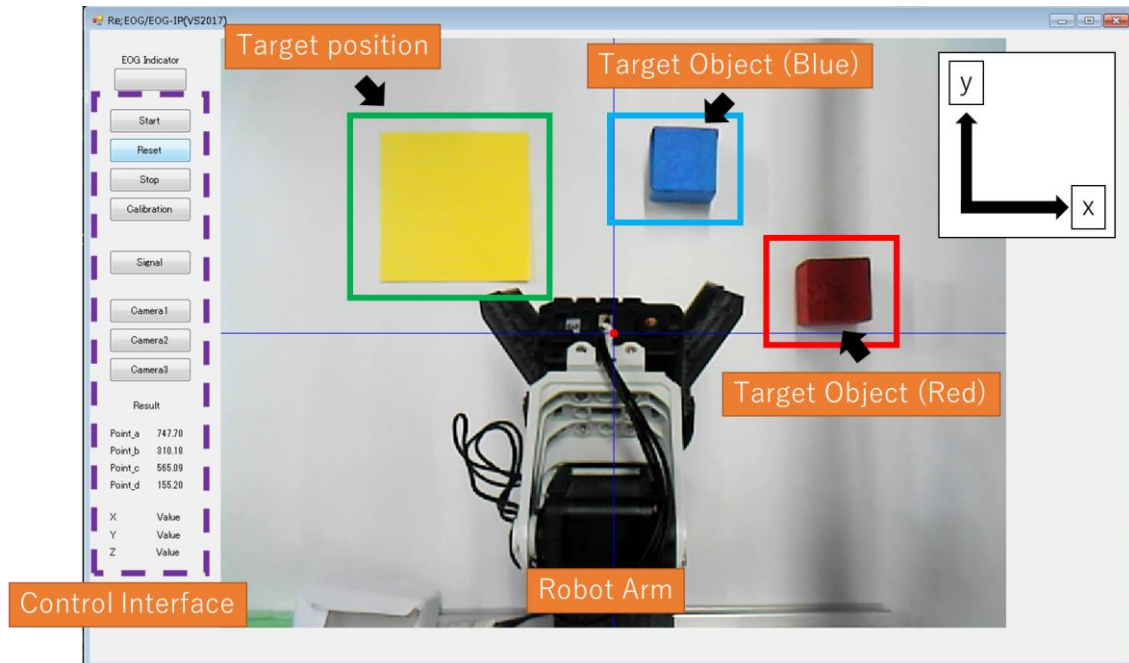


Figure 39. Camera top view

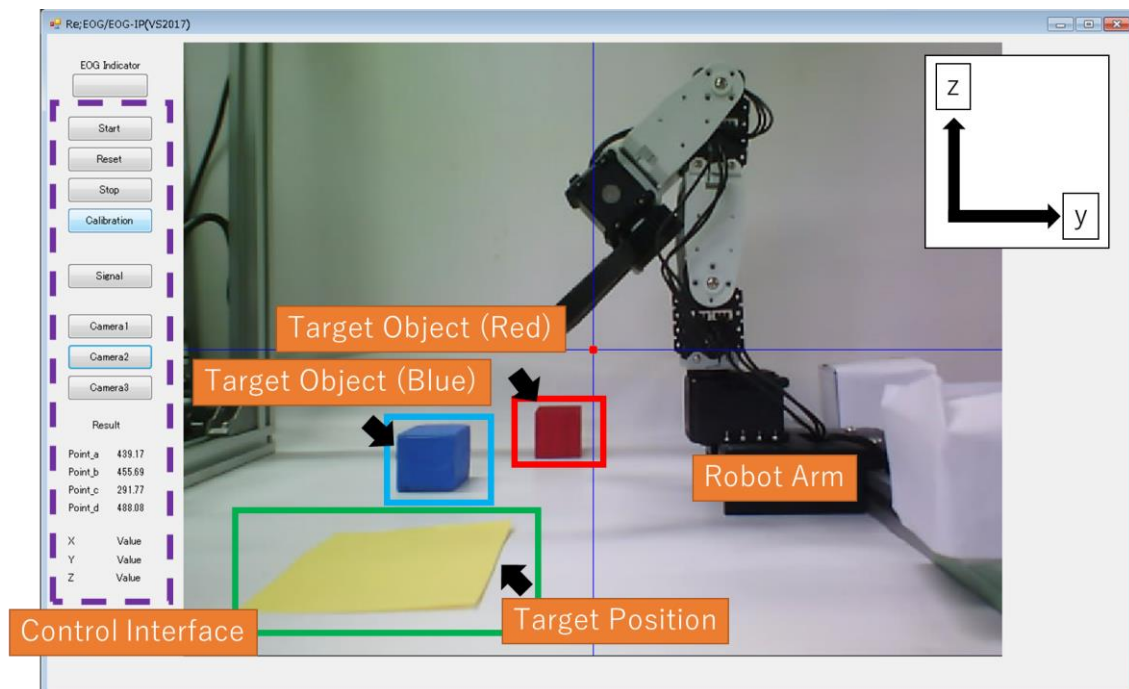


Figure 40. Camera top view

5.2.2. Proposed EOG and EMG robot control method

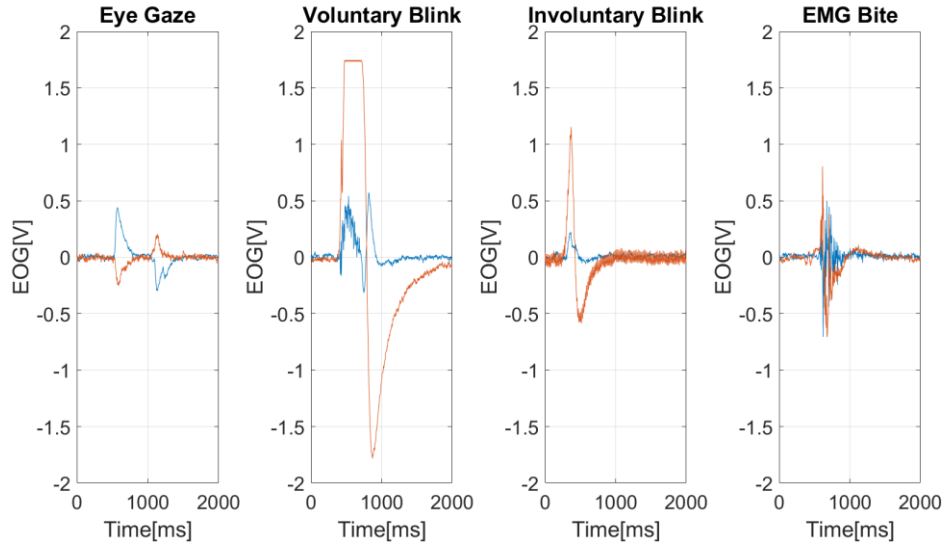


Figure 41. EOG and EMG signal

In this experiment, we are combining the EOG and EMG control method for robot control. Four types of EOG and EMG signals are discriminated for the experiment; eye gaze, voluntary blink, involuntary blink, and EMG bite. Figure 41. Shows the signals used in the experiment.

Each signal has a specific role for the control. For eye gaze, we will discriminate the signal according to gaze direction or gaze estimation, but it shares the same purpose which is to manipulate the robot arm. The two eye blinks; voluntary and involuntary blinks are discriminated, but only involuntary blink is used for camera view control. Voluntary blink served no control in this experiment. Lastly, EMG bite is used for gripper control.

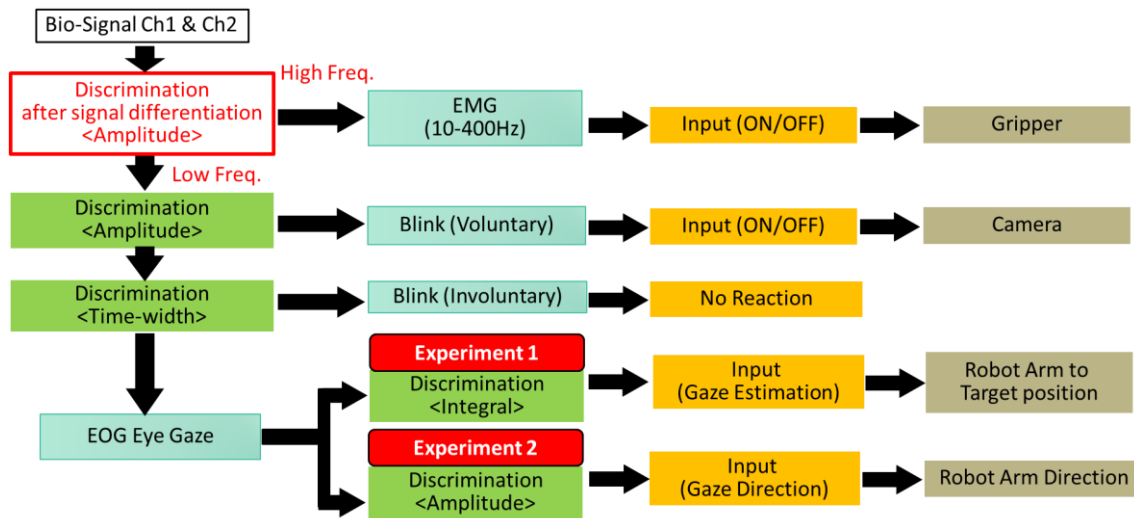


Figure 42. EOG and EMG discrimination algorithm

The signal discrimination algorithm is shown in Figure 42. First, the signal is discriminated against by differential computation to determine whether the signal is an EMG Bite. If the differential maximum amplitude value is more than 0.2, the robot gripper will react. Then, the signal will be discriminated with signal maximum and minimum amplitude value to determine the signal is an involuntary blink. If the amplitude for the Ch2 signal is more than 1.5[v] and less than -1.5[v], involuntary blink is determined.

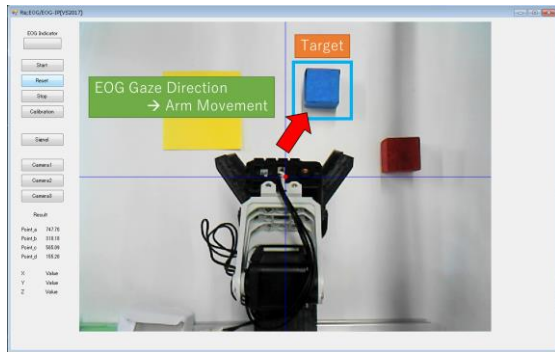
Next, if the signal either EMG bite or involuntary blink, the time width discrimination is used to determine whether the signal is a voluntary blink. If the time-width for Ch2 maximum and minimum amplitude time width is less than 200[ms], the voluntary blink is determined. However, with no reaction for the robot, the signal measurement will restart again.

Finally, the signal is discriminated against for eye gaze. The experiments are divided into two types of EOG eye-gaze control; The gaze direction and gaze estimation. For the EOG gaze direction, the signal is discriminated by the amplitude polarity of Ch1 and Ch2 signals. The robot movement direction is determined by the polarity result. For EOG gaze estimation, on the other hand, signal integral computation is used. The result of the computation is to estimate the eye gazing position on the computer monitor or interface. The position then is used to guide the robot arm movement.

5.2.3. Robot control process

We standardized the process for EOG gaze direction and gaze estimation robot control for each test subject. There are 5 steps in the process for the subject to follow. Figure 43 shows each step in the robot control process in the real-time camera images and the explanation for the steps is as such;

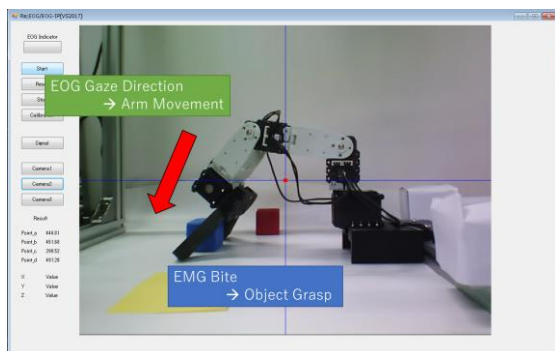
- Step 1: The test subject is required to recognize the position of the target objects, robot arm, and the target position. The initial camera view for the experiment is the top view.
- Step 2: The experiment starts as the test subject moves the robot arm gripper to the target object using the eye gaze.
- Step 3: The test subject then do involuntary eye blinking to change view. The eye gaze is conducted again to move the robot arm gripper closer to the target object. Then, mouth bite to grip the object.
- Step 4: Eye blinking is done again to change view. Then, eye gaze is performed to move the robot arm gripper to the target position.
- Step 5: Eye blinking is done again to change the camera view and finally, mouth bite motion to release the object on the target position.



(a)



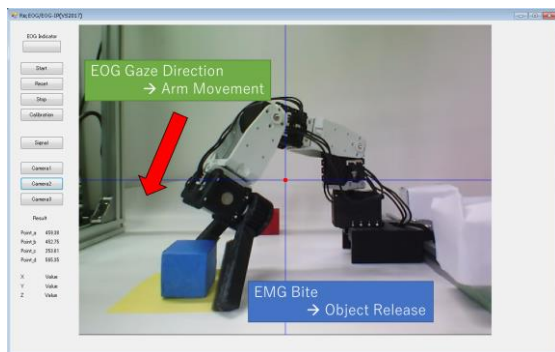
(b)



(c)



(d)



(e)

Figure 43. Robot control task;(a) initial position, (b) robot movement to target object (c) camera view change to grip the object, (d) camera view change for object displacement to target position, (e) Camera view change to release the object to the target position

5.3. Experiment

5.3.1 Investigation on Gaze Estimation Accuracy using Color-based Image processing

The first investigation is to determine the accuracy of gaze estimation. The accuracy is calculated based on the distance between the gaze estimation and the object center point. The distance is represented as an error distance. Two objects have been used; blue and red-colored objects. The object dimension on the camera image is $2 \times 2 \times 2$ [cm] and the object center point is computed by using image processing. Figure 44 shows the process to determine the error distance.

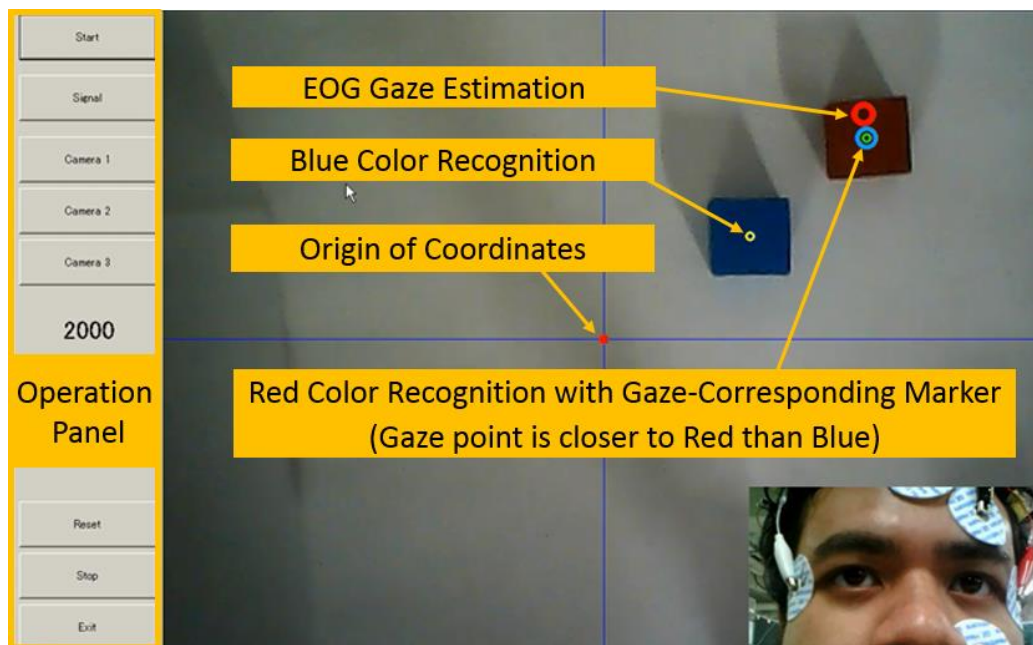


Figure 44. The error distance investigation process; error distance is compute between gaze estimation and object center point.

In this experiment, 100 samples of gaze estimation are taken to determine the error distance. Figure 45 shows the result of the error distance. Based on the result, the blue object has the error distance with the median at 1.865[cm]; maximum value at 5.675[cm] and minimum value at 0.171[cm]. On the other hand, the red object has an error distance with the median at 2.188[cm]; maximum value at 6.985[cm]; and minimum value at 0.1761[cm]. The result also shows that the error distance is approximately in the range of 1.5 to 3.0 [cm]. Based on the error distance, the distance is almost corresponding to the dimension of the object.

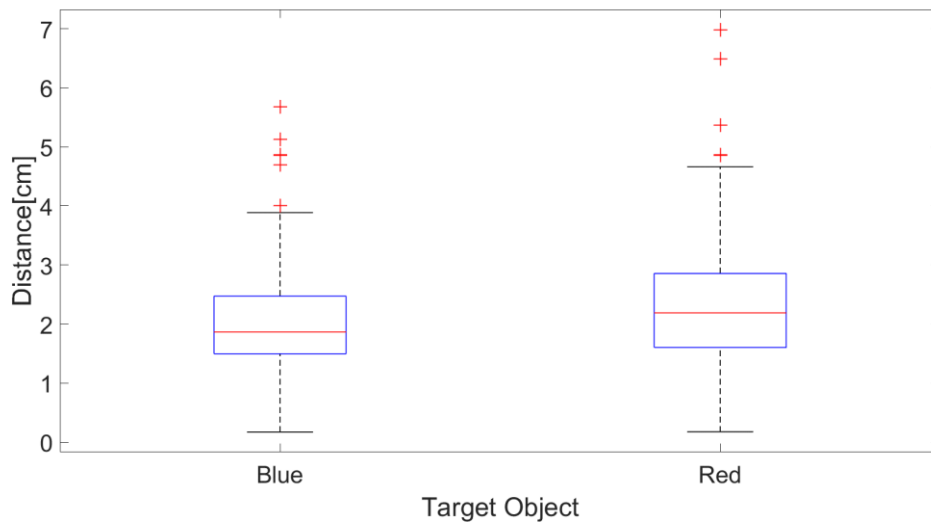


Figure 45. Error distance result between gaze estimation and object center point for 100 samples

5.3.2. Performance Investigation on Gaze Estimation to the Object Displacement Task

In this section, the object displacement task is proposed to investigate the gaze estimation robot control performance. The experiment is conducted three times for each test subject. The color-based image processing is used to compute the target object center point. From the center points, we create a circle using the error distances from the previous experiment as the radius. The circle representing the gaze estimation area for object selection. If the gaze estimation is within the area, the object assumed to be selected and the robot moves to the object center point position.

Two different gaze error distances are proposed for the experiment; 2[cm] and 3 [cm] as additional investigation. The two error distances are to investigate whether control performance is improved with different distances parameter. Figure 46 shows the approximation of the circle area created by the error distances for radius. In this experiment, the task completion time is used as the performance indicator.

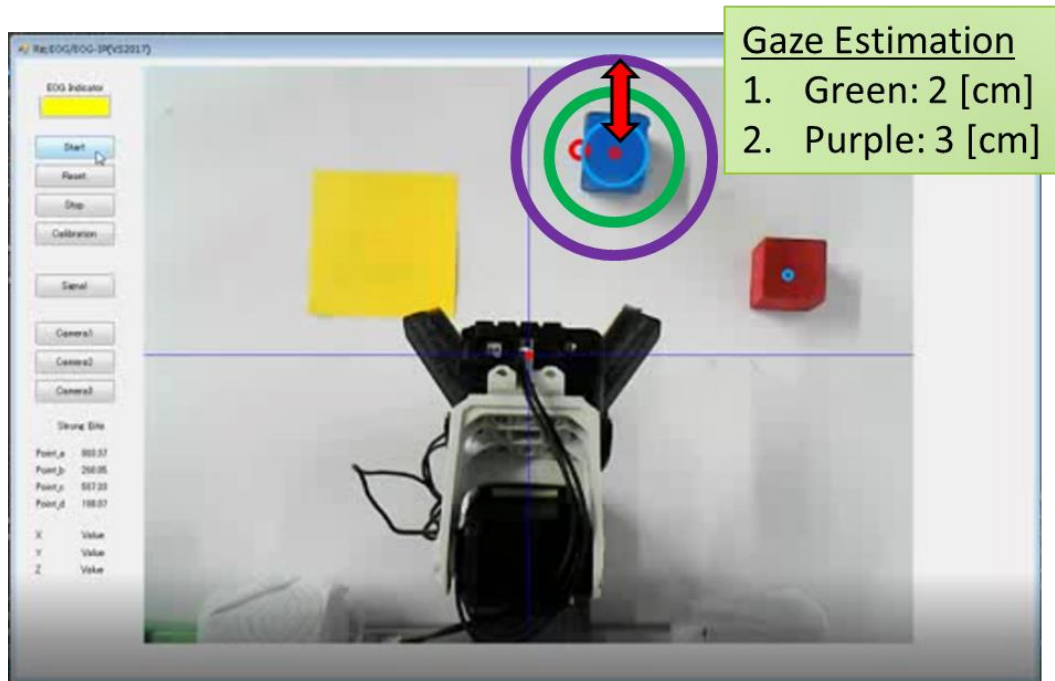


Figure 46. EOG gaze estimation with different gaze error distances; 2[cm] and 3[cm]

Figure 47 shows the examples of EOG and EMG signal for one complete object displacement task and figure 48 shows the concurrent robot x, y, and z-axis position. The gaze estimation result moves the robot to target place in a 2D plane; i.e. x and y plane. However, there is a camera switch function in the control system, the robot able to control in the 3D environment by combining two 2D planes; x and y plane and y and z plane. Based on the graph, there minimal changes in robot x, y, and z-axis positions. As for gaze estimation mainly estimate the eye gaze location, the robot will not move unless the object is confirmed for selection.

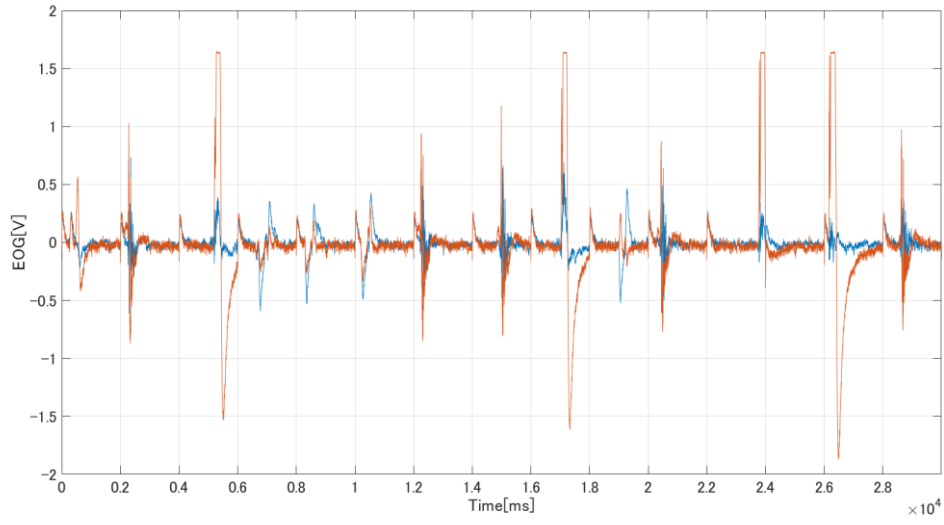


Figure 47. Example of EOG and EMG signals for gaze estimation object displacement task

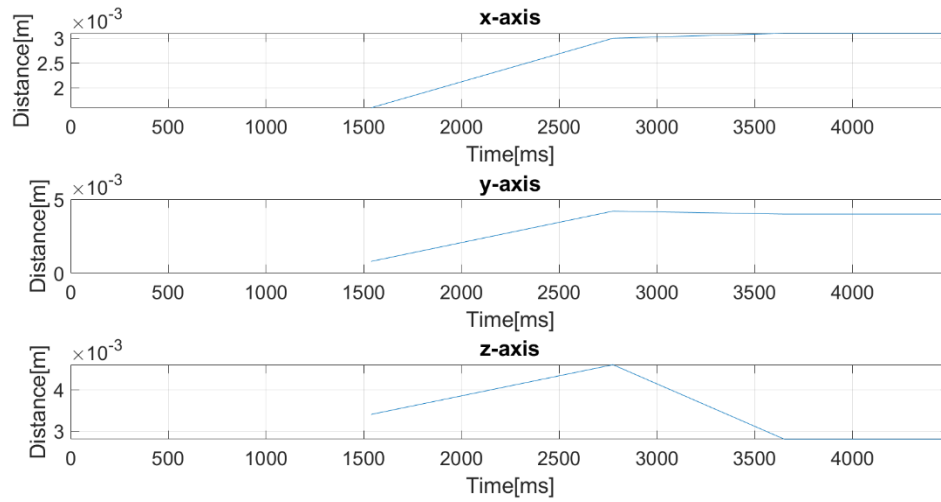


Figure 48. Robot x, y and z-axis movement for gaze direction object displacement

Table 9 shows the completion time for each test subject for three times objects displacement task. Then, figure 49 shows the average of the time completion for each test subject for 2 and 3[cm] error distance. Based on the result, the 3 [cm] is significantly faster than 2 [cm] error distance.

Table 9. Five test subjects completion time for gaze estimation method with two different error distance; 2 and 3[cm]

Test Subject	Test	Error distance 2[cm]		Error distance 3[cm]	
		Time[s]	Average[s]	Time[s]	Average[s]
1	1	36.25	47.89	33.34	31.50
	2	54.79		27.43	
	3	52.63		33.72	
2	1	150.50	84.60	79.72	59.37
	2	65.27		31.57	
	3	38.04		66.83	
3	1	185.31	101.45	85.80	78.52
	2	45.77		86.88	
	3	73.27		62.88	
4	1	49.56	50.17	53.73	48.21
	2	47.49		47.25	
	3	53.47		43.65	
5	1	112.03	69.15	37.93	40.86
	2	50.13		41.93	
	3	45.29		42.71	

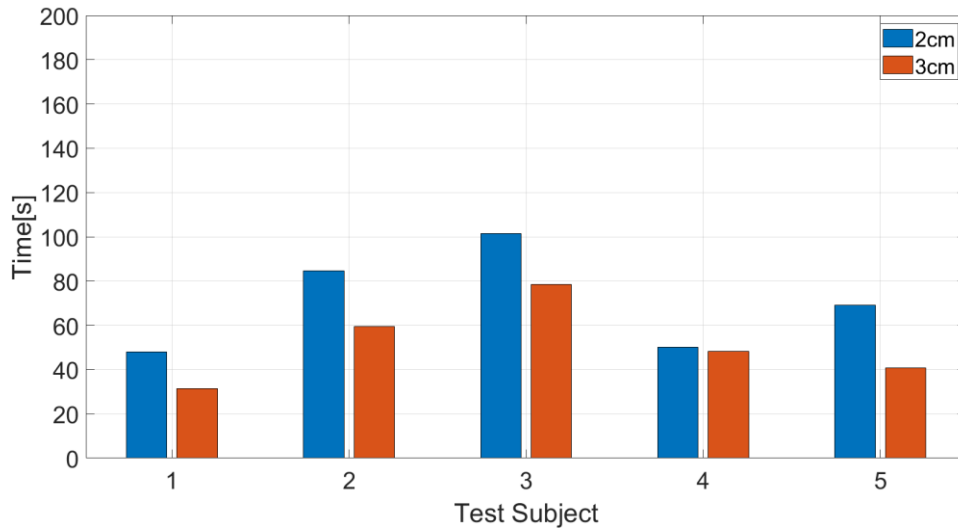


Figure 49. The distribution of average completion time for 5 test subjects with two different error distance; 2 and 3[cm] in gaze estimation methods

Further time analysis has been conducted by computing the average time completion from the test subject to investigate the overall error distance control performance. Figure 50 shows the result. The overall average time completion for 2[cm] gaze error distance is 71[s] and for 3[cm] is 52[s]. From the result, the 3[cm] is significantly 27% faster than 2[cm] gaze error. This shows that the 3[cm] gaze error distance has a better performance for gaze estimation robot control.

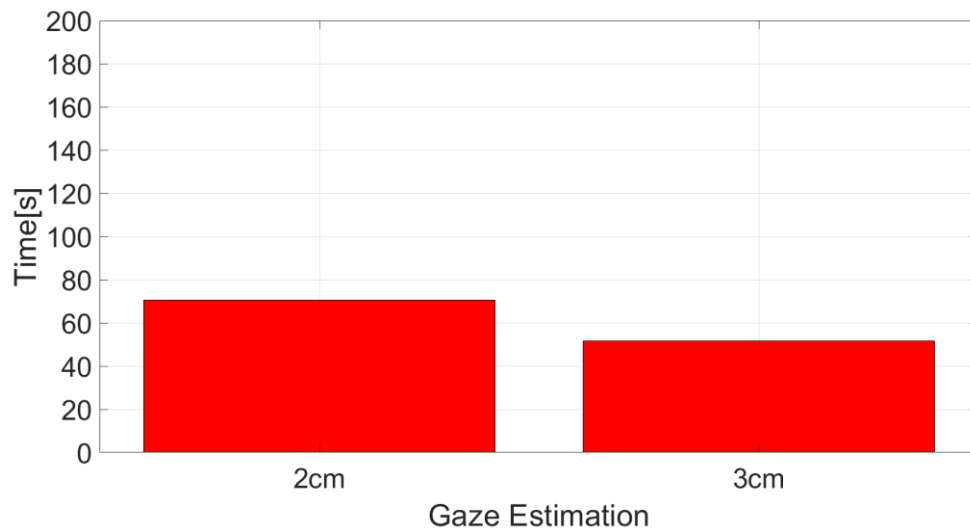


Figure 50. The overall average time completion for 2 and 3[cm] robot movement distances in the gaze estimation method

Experiment feedback is also conducted. All the test subjects commented that the EOG gaze estimation robot control is simple and easy. They commented that they do not felt fatigued and the robot control is fast. However, to select the object, they required high concentration to ensure the gaze estimation near the desired object.

5.3.3. Performance Investigation on Gaze Direction for the Object Displacement Task

For the gaze direction, a similar object displacement task is proposed. The test subjects are instructed to experiment for three times. However, instead of the robot arm moves automatically to the object center point such as gaze estimation control, the gaze direction control the direction of robot arm movement. Each eye gaze direction will navigate the robot arm to the target object position.

Then, there are two distances are used for the robot arm movement; 2 and 3[cm]. Figure 51 shows the approximation of the robot movement distances. The 2[cm] is a fine movement corresponding to object size and the 3[cm] is a slightly expanded movement in which still able to move the robot to the object precisely.

The two distances are proposed to investigate whether the gaze direction control performance could be improved if the movement parameter is changed. The indicator for the control performance is derived by the completion time for the object displacement task.

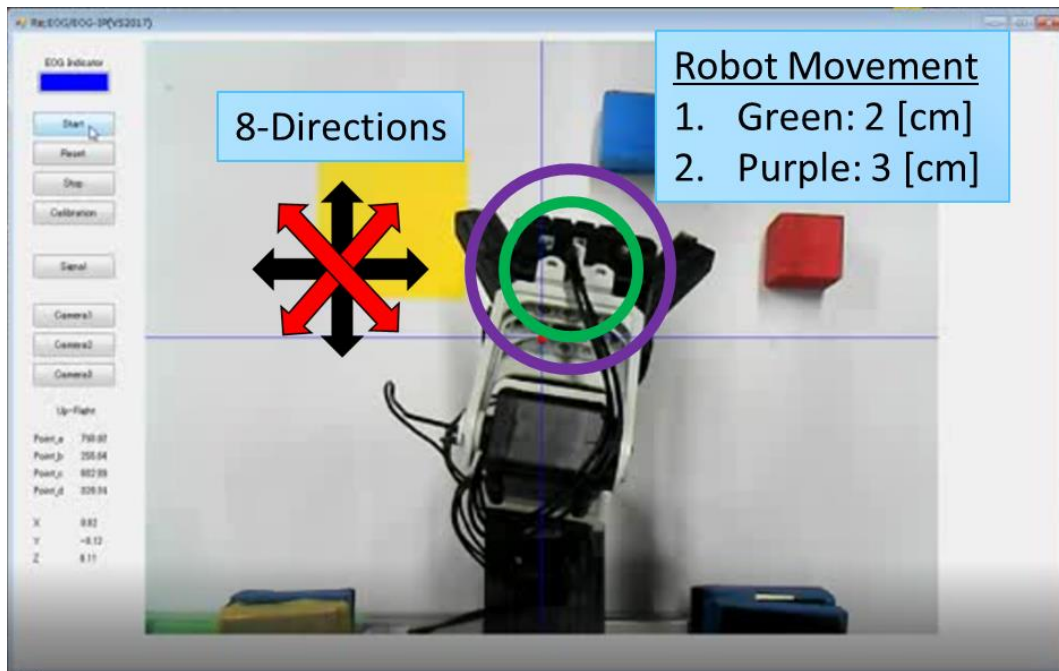


Figure 51. 8-directions EOG gaze direction movement with different robot movement distances; 2[cm] and 3[cm]

Figure 52 shows the examples of EOG and EMG signal for one complete object displacement task and figure 53 shows the concurrent robot x, y, and z-axis position. In this experiment, there are camera-switching functions that enable the 3D control environment. The gaze direction controls the robot according to the 2D movement plane which is x and y plane or y and z plane. The camera-switching function combines these two planes to enable the robot to move in the 3D movement. Based on the figure 46 graph, there a significant change in robot x, y, and z-axis positions. For each of the eye gaze discrimination done, the robot arm will move, thus, changes the x, y, and z-axis position.

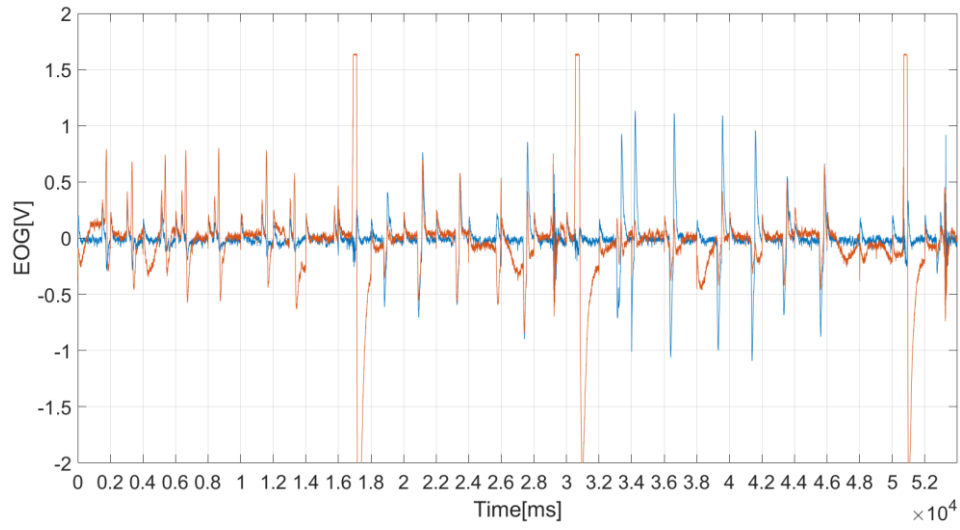


Figure 52. Example of EOG and EMG signals for gaze direction object displacement

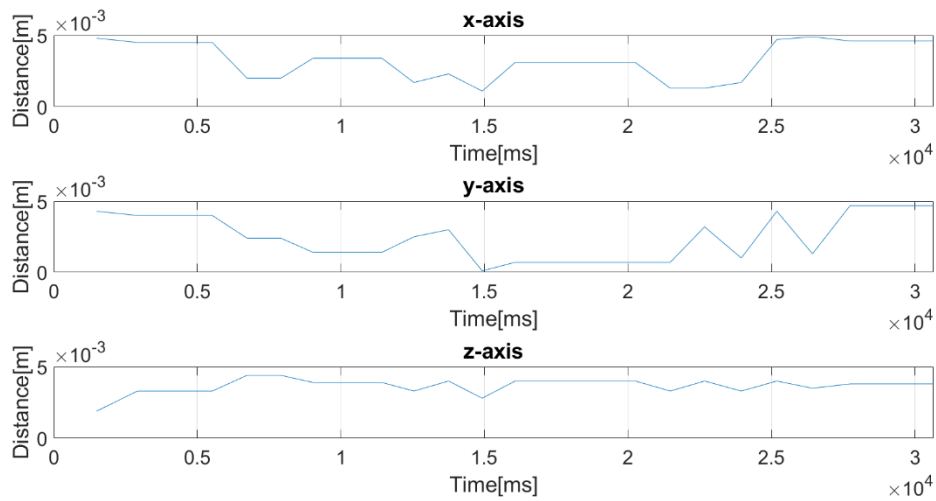


Figure 53. Robot x, y and z-axis movement for gaze direction object displacement

Table 10 and figure 54 shows the time completion result for test subjects to complete the object displacement. Based on the result, each subject 3[cm] robot movement shows a significantly faster time comparing to the 2[cm] robot movement.

Table 10. Five test subjects completion time for gaze estimation control with two different error distance; 2 and 3[cm]

Test Subject	Test	Robot movement 2[cm]		Robot movement 3[cm]	
		Time[s]	Average[s]	Time[s]	Average[s]
1	1	120.87	93.37	54.95	60.96
	2	81.82		75.97	
	3	77.42		51.95	
2	1	186.23	150.62	143.93	117.28
	2	129.40		109.19	
	3	136.22		98.73	
3	1	228.03	183.99	170.93	108.00
	2	169.19		47.00	
	3	154.76		106.08	
4	1	89.52	163.56	118.09	103.27
	2	280.95		94.04	
	3	120.21		97.68	
5	1	243.55	173.68	131.33	126.17
	2	121.16		113.25	
	3	156.32		133.92	

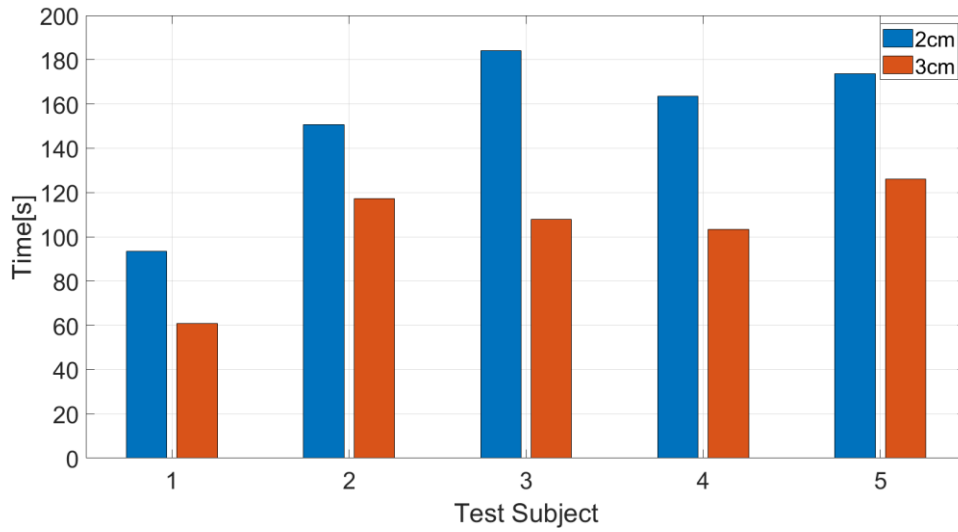


Figure 54. The distribution of average completion time for 5 test subjects with two different error distance; 2 and 3[cm] in gaze direction methods

Overall average time analysis is conducted to determine the control performance for 2 and 3 [cm] robot movement. Figure 55 shows the result. The average time for 2[cm] robot movement distance is 153[s] and for 3[cm] distance is 103[s]. From the average time, the 3[cm] robot movement is 33% faster than 2[cm]. Based on this, the 3[cm] robot movement performed better than 2[cm].

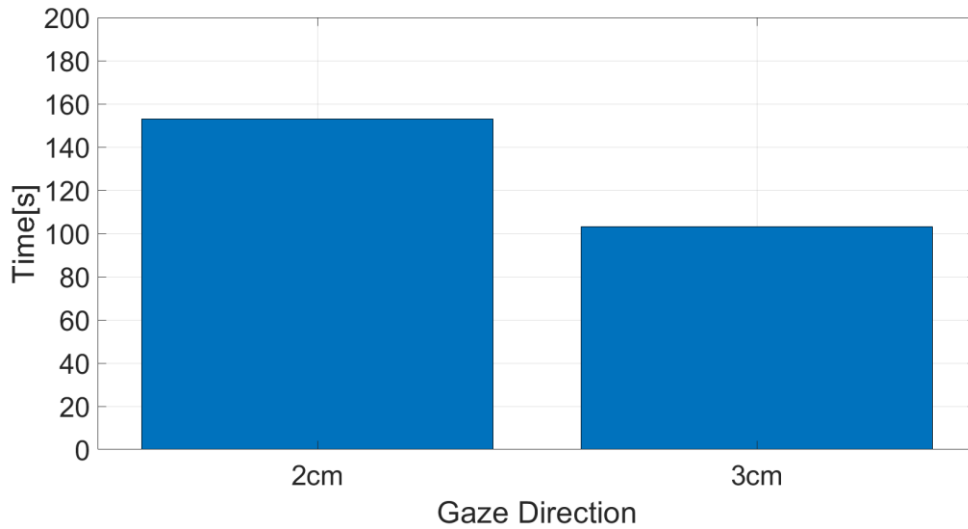


Figure 55. The overall average time completion for 2 and 3[cm] robot movement distances in gaze direction method

Experiment feedback is also conducted. All the test subjects commented that the EOG gaze direction robot control is an arduous task. Each robot movement to destination requires an eye gaze. If a mistake is done, the test subject needs to do movement correction. Then, as the test user needs to wait for the robot movement completed for each eye gaze, the test subjects are easily distracted and get fatigued.

The increasing of the robot movement distance proved to help to improve the gaze direction control. The higher movement distance will reduce the control input requirement. However, if the movement distance is too high; more than 3[cm], the control to aim an object location becomes imprecise. To improve the gaze direction control further, a similar technique as gaze estimation control needs to be implemented. The gaze direction does not control the robot arm directly but instead controls the interface. This means that on the camera interface there are dots or point to indicate the gaze direction. If the gaze direction is performed, the dot will move correspondingly. Only if the dot is on the object, the robot finally will move.

5.3.4. Performance comparison between EOG gaze direction and gaze estimation methods

In this section, we investigate and compare the best EOG eye gaze methods for robot control based on the previous experiment result. There are two indicators used for the comparison, the overall time average and the time distribution in the overall time. Figure 56 shows the time comparison for gaze methods.

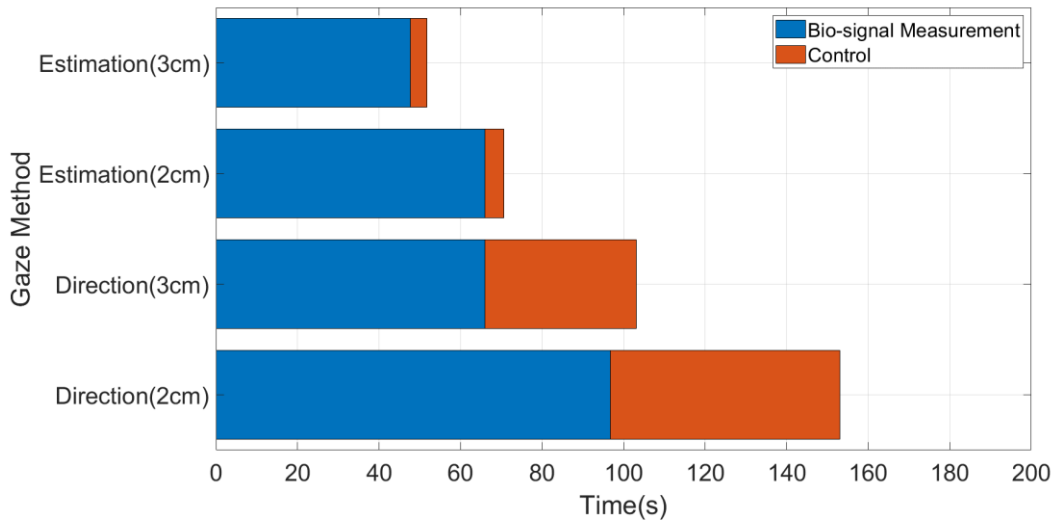


Figure 56. Time distribution for EOG and EMG measurement and robot control time in the Gaze estimation and gaze direction object displacement task

The time average is calculated based on the average for the two distances completion time for the gaze method. Then, there are two types of time distribution inside the overall time average; measurement time and control time. The measurement is the time taken for EOG and EMG measurement. On the other hand, the control time is the time taken to discriminate the signal and compute the robot arm inverse kinematics.

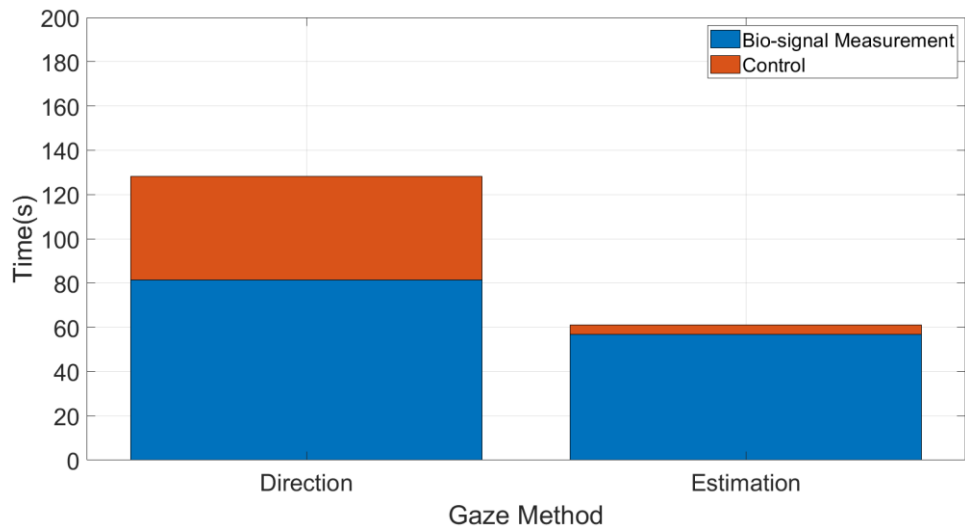


Figure 57. The average time for EOG gaze direction and estimation with the time distribution

Figure 57 shows the combination of both distances time average used for EOG gaze direction and estimation. From the results, the overall time average for gaze estimation is significantly faster compared to the gaze direction. The average time for gaze direction is 128[s] whereas gaze estimation is 61[s]. There is a time difference of 67[s] in which shows that gaze estimation is 52% faster than gaze direction robot control.

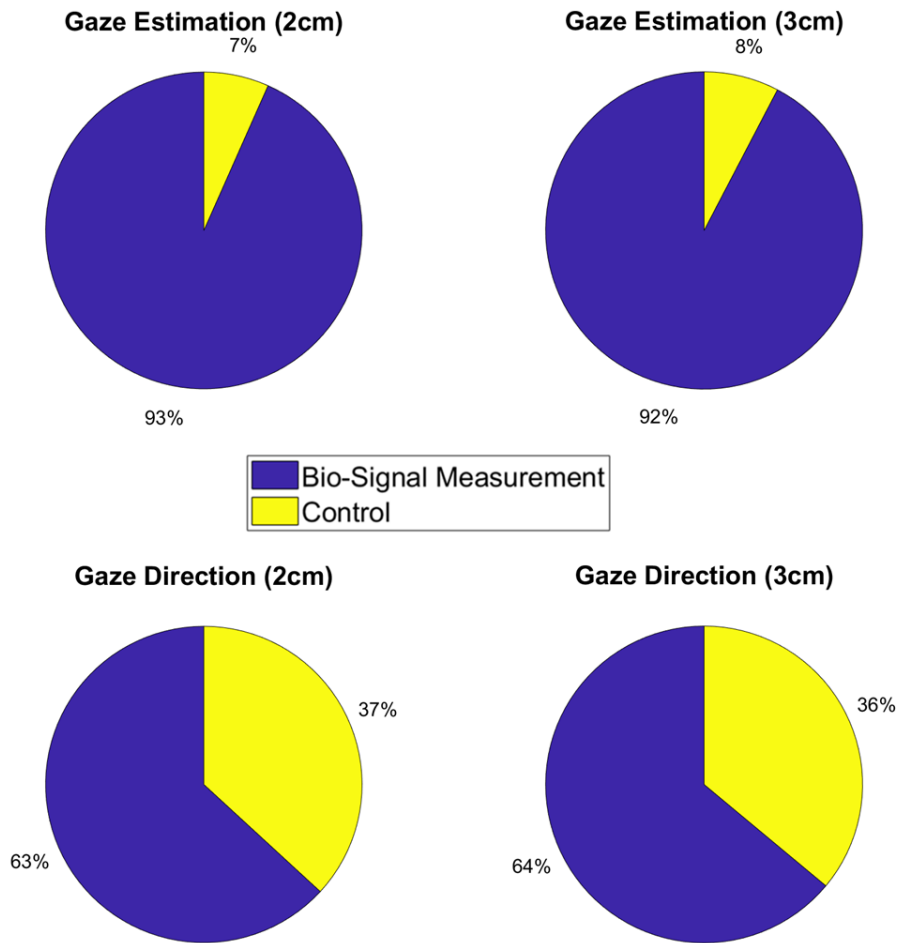


Figure 58. The percentage for measurement and control time distribution.

Then, for the time distribution, the gaze direction control time takes a significantly higher percentage. Figure 58 shows the time distribution percentage for gaze direction and gaze estimation methods. The result indicated that the gaze estimation computation time is less than gaze direction robot control. As to displace an object using the gaze direction method, a significant number of eye gaze need to be performed, followed by the robot arm movement. This increases the computation requirement. However, in the gaze estimation method, the robot only moves if the object is confirmed for selection.

Based on the overall analysis, EOG gaze estimation is the best control method for the robot. The time for object displacement is significantly less than the gaze direction. The computation required is also lesser in which made the method is superior.

5.4. Discussion

In this research, we successfully developed an EOG gaze estimation based robot control with the object recognition to enhance the estimation precision. We also compare the gaze estimation with EOG gaze direction robot control to determine the superior control method. A 3D robot control system is proposed for the gaze methods based object displacement task. The gaze methods are also supported with involuntary eye blink and EMG bite as the control inputs.

Color-based image processing is also implemented to assist the EOG gaze estimation to select an object. The image processing is used to compute the object center point to be compared with the gaze estimation result. In the EOG discrimination, the gaze direction is successfully discriminated against to 8-directions by using maximum and minimum signal amplitude polarity. The gaze estimation is discriminated against by the computation of the signal integral.

The supportive EOG control inputs from eye blinks can be discriminated by the value of the maximum and minimum amplitude value of the Ch2 signal (involuntary blink) and Ch2 signal maximum and minimum amplitude time width (voluntary blink). The voluntary blink has a higher Ch2 signal amplitude than other signals. On the other hand, EMG control inputs from bite motion also successfully discriminated by using the signal differential computation. The EMG produced a differential value higher than EOG eye gaze methods.

Four experiments have been conducted. The first experiment is to determine the

accuracy of gaze estimation with the support of image processing. The accuracy is represented as an error distance between gaze estimation result and computed object center point using image processing. Two specifically colored objects; a red and blue object with a dimension of $2 \times 2 \times 2$ [cm] in camera image has been used. The result shows that the error distance is approximately in the range of 1.5 to 3.0 [cm]. The error distance is approximately similar to the size of the object. The error distance also helps in object selection for the next experiment; object displacement task. By creating the circle area from an object center point using the error distance as the radius, if the gaze estimation is in the area, the object is assumed to be selected and the robot arm will move to the object center point.

The second experiment is to investigate gaze estimation robot control performance in object displacement task. Additional investigation is conducted by using two eye gaze error distances; 2[cm] and 3[cm] to support object selection. This to determine if the control performance improves with different parameters. The completion time is used as the performance indicator. From the result, the 3[cm] robot movement shows the best time. The average time taken for 3[cm] is 52[s] in compare with 71[s] for 2[cm] gaze error. The result shows that 3[cm] is 27% faster. The second experiment also shows that wider gaze error has faster task completion.

The third experiment is to investigate the gaze direction robot control performance. Similarly, object displacement task is proposed and additional investigation is conducted with two robot arm movement distance; 2[cm] and 3[cm]. The different movement distance is investigated to determine if the control performance improved when the movement parameter changed. The task completion time is used as the performance indicator. From the result, the 3[cm] robot movement shows the best time. The 3[cm]

average time taken is 103[s] compared to 153[s] for 2[cm] robot movement. This shows 3[cm] is 33% faster than 2[cm] gaze direction robot movement. Based on the experiment, the larger the robot movement distance, the quicker the task completion.

The forth experiment is to compare the two gaze methods to determine which gaze method is the best for robot control. The time average and time distribution in which indicate the EOG and EMG measurement (measurement time) and robot control (control time) is used as an indicator. Based on the analysis, the gaze estimation is the best robot control method. The gaze estimation time taken is 52% faster than the gaze direction. For the time distribution, the gaze estimation based control required significantly less computation time for robot movement. The percentage for control time is at 8% compared to gaze direction at 36%. These differences make gaze estimation robot control is a simple and superior method.

Chapter 6

Conclusion

There are three objectives of this research. For the first objective, we are enhancing the EOG measurement stability using a custom-made EOG mask. The proposed mask manufacturing process is to acquire a 3D face model with a 3D scanner and to modify the model to the design of the mask, and to build the mask with a 3D printer. An investigation on EOG signal stability is conducted to compare the conventional manual hand electrode placement and the proposed method. Based on the eye gaze direction(up, down, right, and left) signal experiment, both methods show similarities in signal patterns. As for the signal maximum amplitude value, we observed a minimal inconsistency for the EOG mask. Then, standard deviation computation is conducted. The EOG mask shows significantly better standard deviation results. From the overall analysis, the EOG mask not only is simple and quick for EOG signal measurement, but the signal is also more stable than the conventional electrode placement method.

The second objective of the research was to enhance the accuracy of the EOG gaze estimation method using the calibration method. We proposed the conversion method for 24-point gazing data simultaneously and assumed a virtual origin (i.e., 25th point) on gaze coordinates with 24-point gazing data and applied an affine transformation to 24-point gazing data. Two experiments were conducted as a comparative investigation for the conventional and proposed methods. The first experiment was an accuracy investigation between the proposed method and conventional computation. The result shows that the

proposed method achieved negligible error in gazing data conversion. The second experiment was to determine the accuracy of the proposed method using EOG gazing data. Ten test subjects were used to performed 24-point gaze targets with two different electrode attachment methods. The average angle error for the cross-shaped electrode attachment was $x=2.27^{\circ}\pm0.46^{\circ}$ and $y=1.83^{\circ}\pm0.34^{\circ}$. On the other hand, the plus-shaped electrode attachment had an error of $x=0.94^{\circ}\pm0.19^{\circ}$ and $y=1.48^{\circ}\pm0.27^{\circ}$. The results show that there was a minimal error using the proposed method. From the experiments, the proposed method was simpler and more accurate in EOG gaze estimation.

The third objective is to compare which EOG gaze method; EOG gaze direction or gaze estimation performs better. A 3D robot control system is proposed for the gaze methods for an object displacement task. The gaze methods are also supported with involuntary eye blink and EMG bite as the control inputs. Color-based image processing is also implemented to assist the EOG gaze estimation to select an object. The image processing is used to compute the object center point to be compared with the gaze estimation result.

Four sub experiments have been conducted. The first sub experiment is to determine the accuracy of gaze estimation with the support of image processing. The accuracy is represented as an error distance between gaze estimation result and computed object center point using image processing. Two specifically colored objects; red and blue objects have been used. The result shows that the error distance is approximately in the range of 1.5 to 3.0 [cm]. The error distance is then used to create the circle area from the object center point. If the gaze estimation is in the circle area, the object is assumed to be selected and the robot arm will move to the object center point.

The sub second experiment is to investigate gaze estimation robot control performance in object displacement task. Two eye gaze error distances are proposed; 2[cm] and 3[cm] as additional investigation. The two error distances are investigated to determine if the control performance improved with different error distance parameter. The completion time is used as the performance indicator. From the result, the 3[cm] robot movement shows the best time. The average time taken for 3[cm] is 52[s] in compare with 71[s] for 2[cm] gaze error. The result shows that 3[cm] is 27% faster. The second experiment also shows that wider gaze error has faster task completion.

The third sub experiment is to investigate gaze direction robot control performance. The object displacement task is proposed and additional investigation proposed with two robot arm movement distances; 2[cm] and 3[cm]. The two robot movement distances are investigated to determine if the control performance improved when the movement distance changed. The task completion time is used as the performance indicator. From the result, the 3[cm] robot movement shows the best time. The 3[cm] average time taken is 103[s] compared to 153[s] for 2[cm] robot movement. This shows 3[cm] is 33% faster than 2[cm] gaze direction robot movement. Based on the experiment, the larger the robot movement distance, the quicker the task completion.

The fourth sub experiment is to compare the two gaze methods to determine which gaze method is the best for robot control. From the second and third experiments, the overall time average is investigated for the gaze methods performance comparison. An additional investigation from the overall time in which time distribution EOG and EMG measurement (measurement time) and robot control (control time) used for the performance comparison. Based on the investigation, gaze estimation is the best robot control method. The gaze estimation time taken is 52% faster than the gaze direction. For

the time distribution, the gaze estimation method required significantly less computation time for robot movement. The percentage for control time is at 8% compared to gaze direction at 36%. These differences make gaze estimation robot control is a simple and superior method.

List of References

1. Arden; G. B.; Constable, P. A.. The electro-oculogram. *Prog. Retin. Eye Res.* 2006, 25, 207–248.
2. Venkataramanan, S.; Nemade, H.B.; Sahambi, J.S. Design and development of a novel EOG bio-potential amplifier. *Int. J. Bioelectromagn.* 2005, 7, 271–274
3. Manabe, H.; Fukumoto, M.; Yagi, T. Direct gaze estimation based on nonlinearity of EOG. *IEEE Trans. Biomed. Eng.* 2015, 62, 1553–1562.
4. Yagi, T.; Kuno, Y.; Koga, K.; Mukai, T. Drifting and blinking compensation in electro-oculography (EOG) eye-gaze interface, In *Proceedings of the 2006 IEEE International Conference on Systems, Man and Cybernetics*, Taipei, Taiwan, 8-11 October 2006; pp. 3222–3226.
5. Sakurai, K.; Yan, M.; Tanno, K.; Tamura, H.; Gaze Estimation Method Using Analysis of Electrooculogram Signals and Kinect Sensor. *Comput. Intell. and Neurosci.* 2017, 2017, doi:10.1155/2017/2074752
6. Yan, M.; Tamura, H.; Tanno, K. A study on gaze estimation system using cross-channels electrooculogram signals. In *Proceedings of the International MultiConference of Engineers and Computer Scientists*, Hong Kong, China, 12–14 March 2014; pp. 112–116.
7. S. Aung Sakul, A. Phinyomark, P. Phukpattaranont, C. Limsakul, Evaluating Feature Extraction Methods of Electrooculography (EOG) Signal for Human-Computer Interface, *Procedia Engineering* 32, pp 246 – 252, 2012

8. Muhammad Ilhamdi Rusydi, Minoru Sasaki, Satoshi Ito, Calculate Target Position of Object in 3-Dimensional Area Based on the Perceived Locations Using EOG Signals, JCC, Vol.2, No.11, pp. 53-60,2014
9. Rusydi, M.I.; Okamoto, T.; Ito, S.; Sasaki, M. Rotation Matrix to Operate a Robot Manipulator for 2D Analog Tracking Objects Using Electrooculography. *Robotics* 2014, 3, 289–309.
10. Rusydi, M.I.; Sasaki, M.; Ito, S. Affine Transform to Reform Pixel Coordinates of EOG Signals for Controlling Robot Manipulators Using Gaze Motions. *Sensors* 2014, 14, 10107–10123
11. Postelnicu, C.C.; Girbacia, F.; Talaba, D. EOG-based visual navigation interface development. *Expert Syst. Appl.* 2012, 39, 10857–10866.
12. Lledó, L.D.; Úbeda, A.; Iáñez, E.; Azorín, J.M. Internet browsing application based on electrooculography for disabled people. *Expert Syst. Appl.* 2013, 40, 2640–2648.
13. Trieu T.H. Pham, Rodney J. Croft , Peter J. Cadusch, Robert J. Barry, A test of four EOG correction methods using an improved validation technique, *International Journal of Psychophysiology* 79, pp 203–210, 2011
14. Lawrence Y. Deng, Chun-Liang Hsu, Tzu-Ching Lin, Jui-Sen Tuan, Shih-Ming Chang, EOG-based Human–Computer Interface system development, *Expert Systems with Applications* 37, pp. 3337–3343, 2010
15. FANG WenShan, Itakura Naoaki, Evaluation for measurement of continual eye-gaze shift for the eye-gaze input interface using electro-oculogram amplified by AC coupling : comparison with limbus tracking method, *IEICE technical report* 106(285), 41-44, 2006-10-05

16. R. Barea, L. Boquete, S. Ortega, E. López, J.M. Rodríguez-Ascariz, EOG-based eye movements codification for human computer interaction, *Expert Systems with Applications* 39, pp 2677–2683, 2012
17. Cristian-Cezar Postelnicu, Florin Girbacia, Doru Talaba, EOG-based visual navigation interface development, *Expert Systems with Applications* 39, pp 10857–10866, 2012
18. Zhao Lv, Xiao-pei Wua, Mi Li, Dexiang Zhang, A novel eye movement detection algorithm for EOG driven human computer interface, *Pattern Recognition Letters* 31, pp 1041–1047, 2010
19. Wen-Tsai Sung, Jui-Ho Chen, Kuo-Yi Chang, ZigBee based multi-purpose electronic score design and implementation using EOG, *Sensors and Actuators A* 190, pp 141–152, 2013
20. Eduardo Iáñez, Andrés Úbeda, José M. Azorín, Carlos Perez-Vidal, Assistive robot application based on an RFID control architecture and a wireless EOG interface, *Robotics and Autonomous Systems* 60, pp 1069–1077, 2012
21. Muhammad Ilhamdi Rusydi, Control of robot manipulator using electrooculography, pp 12-40, 2014.
22. Muhammad Ilhamdi Rusydi , Minoru Sasaki , Satoshi Ito, Affine Transform to Reform Pixel Coordinates of EOG Signals for Controlling Robot Manipulators Using Gaze Motions, *Sensors*, Volume 16, Issue 6, pp 10107-10123, 2014.
23. Sasaki Minoru, Ito Satoshi, Takeda Koichi, OKAMOTO Takeo, Muhammad Ilhamdi Rusydi, Developing a two-link robot arm controller using voluntary blink., *Journal of the Japan Society of Applied Electromagnetics and Mechanics* 22(4), 475-481,

2014

24. R. BAREA, L. BOQUETE, M. MAZO and E. LÓPEZ, Wheelchair Guidance Strategies Using EOG, *Journal of Intelligent and Robotic Systems* 34, pp279–299, 2002,
25. A. Naga Rajesh, S. Chandralingam, T. Anjaneyulu, K. Satyanarayana, EOG Controlled Motorized Wheelchair for Disabled Persons, *International Journal of Medical, Health, Biomedical, Bioengineering and Pharmaceutical Engineering* Vol:8, No:5, pp 302-305, 2014
26. Gibaldi, A; Vanegas, M; Bex, P.J.; Maiello, G. Evaluation of the Tobii EyeX Eye tracking controller and Matlab toolkit for research. *Behav. Res. methods* 2017, 49, 923–946
27. Lim, Y.; Gardi, A.; Pongsakornsathien, N.; Sabatini, R.; Ezer, A.; Kistan, T. Experimental characterisation of eye-tracking sensors for adaptive human-machine systems. *Measurement* Volume 2019, 140, 151–160.
28. Yasui, Y.; Tanaka, J.; Kakudo, M.; Tanaka, M.. Relationship between preference and gaze in modified food using eye tracker. *J. Prosthodont. Res.* 2019, 63, 210–215.
29. Takahashi, R.; Suzuki, H.; Chew, J.Y.; Ohtake, Y.; Nagai, Y.; Ohtomi, K. A system for three-dimensional gaze fixation analysis using eye tracking glasses, *J. Comput. Des. Eng.* 2018, 5, 449–457.
30. Al-Rahayfeh, A.; Faezipour, M. Eye Tracking and Head Movement Detection: A State-of-Art Survey. *IEEE J. Transl. Eng. Health Med.* 2013, 1, 2100212–2100212, doi:10.1109/JTEHM.2013.2289879.
31. Blignaut, P.; van Rensburg, E.J.; Oberholzer, M. Visualization and quantification of eye tracking data for the evaluation of oculomotor function. *Heliyon* 2019, 5, e01127.

32. Deng, L.Y.; Hsu, C.-L.; Lin, T.-C.; Tuan, J.-S.; Chang, S.-M. EOG-based human–computer interface system development. *Expert Syst. Appl.* 2010, 37, 3337–3343.
33. 11. Chen, Y.; Newman; W. S. A human–robot interface based on electrooculography. In *Proceedings of the IEEE International Conference on Robotics and Automation*, New Orleans, LA, USA, 26 April–1 May 2004; pp. 243–248.

List of Publications

Journal

1. Minoru Sasaki, **Muhammad Syaiful Amri bin Suhaimi**, Kojiro Matsushita, Satoshi Ito, Muhammad Ilhamdi Rusydi, Robot Control System Based on Electrooculography and Electromyogram, Journal of Computer and Communications, 2015, 3, 113-120, doi: 10.4236/jcc.2015.311018.
2. **Muhammad Syaiful Amri bin Suhaimi**, Kojiro Matsushita; Minoru Sasaki, Waweru Nyeri. 24-Gaze-Point Calibration Method for Improving the Precision of AC-EOG Gaze Estimation. Sensors 2019, 19, 3650. <https://doi.org/10.3390/s19173650>

Conference

1. **Muhammad Syaiful Amri bin Suhaimi**, Kojiro Matsushita, Minoru Sasaki, Development of Custom-made EOG Glasses based on 3D Face Scanning, Japan Design Engineering Society Spring Meeting Research Presentation Conference, May 2017, pg. 33-34
2. **Muhammad Syaiful Amri bin Suhaimi**, Kojiro Matsushita, Minoru Sasaki, Development of EOG and EMG based Interface for Robot Control, The Society of Instrument and Control Engineers(SICE) Chubu branch Young Researcher Presentation, November 2018.

3. **Muhammad Syaiful Amri bin Suhaimi**, Kojiro Matsushita, Minoru Sasaki, Robot arm control based on combination of bio-signal analysis (EOG and EMG) & Image Analysis (Deep Learning, etc), IEEE Nagoya YP Workshop, December 2018.
4. S. M. Namal Arosha Senanayake, Nursyuhada Hj Kadir, **Muhammad Syaiful Amri bin Suhaimi**, Minoru Sasaki, Master-Slave IoT for Active Healthy Life Style, 12th IEEE International Conference on Human System Interaction, June 2019, RF-000728.
5. Minoru Sasaki, Kojiro Matsushita, Muhammad Ilhamdi Rusyidi, Pringgo Widyo Laksono, Joseph Muguro, **Muhammad Syaiful Amri bin Suhaimi**, Waweru Njeri, Robot Control Systems Using Bio-Potential Signals, The 5th International Conferences of International Conference on Industrial, Mechanical, Electrical, and Chemical Engineering (ICIMECE 2019), September 2019.
6. Pringgo Widyo Laksono, Minoru Sasaki, Kojiro Matsushita, **Muhammad Syaiful Amri bin Suhaimi**, Joseph Muguro, Preliminary Research of Surface Electromyogram (sEMG) Signal Analysis for Robotic Control Arm, The 5th International Conferences of International Conference on Industrial, Mechanical, Electrical, and Chemical Engineering (ICIMECE 2019), September 2019, EE-057.

7. Joseph Muguro, Minoru Sasaki, Kojiro Matsushita, Waweru Nyeri, Pringgo Widyono Laksono, **Muhammad Syaiful Amri bin Suhaimi**, Human-Machine Interface for game Control Using Neck SEMG Signal, The 5th International Conferences of International Conference on Industrial, Mechanical, Electrical, and Chemical Engineering (ICIMECE 2019), September 2019, EE-066. (Best Paper award)